POLITEHNICA University of Bucharest
FACULTY OF MATERIALS SCIENCE AND ENGINEERING
București, Splaiul Independenței, nr. 313, Sector 6, cod poștal 060042
http://www.sim.pub.ro

PhD Thesis Summary

Specific Aspects Concerning the Behaviour of Some Super Duplex Stainless Steel Alloys during Thermomechanical Processing

Author: Saleh Sabah Saleh ALTURAIHI

Scientific coordinator: Prof. Habil. Dr. Eng. Vasile Dănuț COJOCARU

DOCTORAL COMMITTEE

President	Prof. Habil. Dr. Eng. Constantin Stelian STAN	From	POLITEHNICA University of Bucharest
Scientific supervisor	Prof. Habil. Dr. Eng. Vasile Dănuț COJOCARU	From	POLITEHNICA University of Bucharest
Scientific reviewer	Prof. Dr. Eng. Leandru-Gheorghe BUJOREANU	From	Gheorghe Asachi Technical University of Iasi
Scientific reviewer	Prof. Dr. Eng. Anna NOCIVIN	From	OVIDIUS University of Constanta
Scientific reviewer	Prof. Dr. Eng. Doina RADUCANU	From	POLITEHNICA University of Bucharest

Bucharest, 2022

POLITEHNICA University of Bucharest
FACULTY OF MATERIALS SCIENCE AND ENGINEERING
Bucureşti, Splaiul Independenţei, nr. 313, Sector 6, cod poştal 060042
http://www.sim.pub.ro

Table of Contents

Abstract

In this thesis, different experimental programs were developed aiming to design appropriate thermomechanical processing routes to correlate the effects induced by thermomechanical processing on the microstructure and mechanical properties of Super Duplex Stainless Steel (SDSS) F55 alloy, to obtain an appropriate combination of strength and ductility properties. The developed experimental programs show a high level of complexity. The processing routes were based on the following main parameters: the deformation temperature of SDSS F55 alloy, in the range of 1000°C to 1150°C, the solution treatment temperature, in the range of 1000°C to 1100°C and, the solution treatment duration, in the range of 20min to 60min. Hot deformation at 1000°C and 1050°C lead to a microstructure containing Ferrite (δ), Austenite (γ) and Sigma (σ) phases. Hot deformation at temperatures above 1100°C lead to a microstructure containing only Ferrite (δ) and Austenite (γ) phases, the Sigma (σ) phase being dissolved from the SDSS F55 alloy microstructure. Applying a solution treatment at 1000°C leads to Sigma (σ) phase precipitation within the SDSS F55 alloy microstructure, while at solution treatments above 1050°C the Sigma (σ) phase disappeared from the microstructure. The mechanical properties obtained by tensile (0.2 Yield Strength, Ultimate Tensile Strength and Elongation to fracture) and microhardness (HV0.1) testing are suffering changes depending on the applied thermomechanical processing route. The fracture surfaces obtained after tensile testing were examined in order to determine the SDSS F55 alloy fracture behaviour.

Keywords: Super duplex stainless steel alloy; Microstructure; Mechanical properties; Thermomechanical processing; Fracture surface; Optical microscopy; Scanning electron microscopy.

Chapter 1: Introduction

1.1. Overview

The stainless steels are iron-based alloys consisting of almost 11% of chromium, with the role of preventing rusting and, also, to give heat resistant properties [1]. Stainless-steel alloys contain small quantities of carbon, sulphur, copper, niobium, molybdenum, aluminium, silicon, titanium, nickel and selenium [2]. Some stainless-steel alloys are frequently assigned in three digits numbers, e.g., 304 stainless steel [3]. The existence of chromium in the alloy microstructure prevents the formation of surface oxides, which can generate an unfavourable surface layer increasing the corrosion rate [4].

Corrosion resistance could be raised by raising the content of the chromium, above 11%, the content of nickel, up to 8% or higher, and the content of molybdenum, all improving the stainless-steel alloy pitting corrosion resistance. Adding nitrogen can increase the pitting corrosion resistance and, also, raises the mechanical strength.

The history of stainless steel alloys development started in 1798 when Louis Vauquelin presented chromium to the French Academy. At the beginning of the 1800's James Stoddart, Robert Mallet and Michael Faraday proved that the resistance to oxidizing agents can be increased by adding chromium to the steel composition, due to Robert Bunsen's discovery in 1821 that showed that chromium possesses a high resistance to strong acids. The resistance to corrosion of iron-chromium alloys was observed also by Pierre Berthier, which recommended their potential use in the cutlery industry. Standardized chromium-containing steels were produced in 1840's by Sheffield and Krupp steelmakers and were used in canon constructions since 1850's [5].

Due to their corrosion resistance, the steels containing chromium were firstly used in the civil industry (buildings and bridge constructions) by J. Baur in Brooklyn. In 1869 the first patent for a chromium alloy product was issued in USA. After that, John Clark and Englishmen J.T. Woods researched besides chromium the addition of tungsten in order to improve alloy's corrosion resistance. Hans Goldschmidt, in 1890's, researched the aluminothermic operation to produce carbon-free chromium. Between 1904-1911 many researchers, such as Leon Guillet, investigated some alloys that today would be recognised as stainless-steel alloys.

Chapter 2: Metallurgical aspects of stainless steels and their applications

2.1. Introduction

definition, super duplex stainless steels are a group of iron-based alloys that consist of almost equal fractions of ferrite (δ-Fe) phase, as a matrix, and austenite (γ-Fe) phase.

The chemistry of the duplex stainless steel governs the weight fraction of the constituent ferrite (δ-Fe) and austenite (γ-Fe) phases [14]. The weight fraction combination of ferrite – austenite phases can be obtained by mixing different quantities of ferrite/austenite stabilizing elements. Molybdenum and chromium are active as ferrite stabilizers, generating a large ferrite forming range in the alloy's phase diagram. Generally, the ferrite phase is considered the dominant phase and is showing good mechanical and corrosion resistance, due to its increased content of chromium. Chromium is considered one of the most significant alloying elements within stainless steel composition due to its ability to generate a passive film of Cr_2O_3 on alloy surfaces [15].

2.2. Classification of Duplex Stainless Steels

Duplex stainless steel can be classified into many classes, considering the weight fraction of the alloy elements, which are playing a major role in the alloy's corrosion resistance. Normally, the designation of the duplex stainless steel is in four numbers: the initial two numbers show the volume fraction of Cr and, the second two numbers show the volume fraction of Ni. Thus, 2507 duplex stainless steel presents a volume fraction 25%Cr and 7%Ni. Besides this, many types of duplex stainless steel contain registered designation trademarks, like Uranus 50, Ferralium 255 and Zeron 100. By Nilsson [28], the duplex stainless steels can be categorized into four main classes:

2.2.1 Low Alloyed
2.2.2 Medium Alloyed
2.2.3 High Alloyed
2.2.4 Super Duplex Stainless Steels

2.6 Duplex stainless steels: some use areas

2.6.1 Oil Production:

- Heat exchangers
- Crude Distillation
- Hydrotreating

2.6.2 Petrochemicals
2.6.3 Desalination plants
2.6.4 Automotive Applications

Chapter 3: Thermomechanical processing of stainless-steel alloys.

3.1. Introduction

This chapter is focused on the mechanical and thermal processing steps/operations that may be applied to the stainless steel alloys. The major mechanical and thermal processing operations are shown in this chapter to give ground for understanding the induced changes during an applied thermomechanical processing cycle, in terms of microstructural and mechanical behaviour [79].

Chapter 4: Problem statement and objectives.

4.1. Problem statement

Numerous researchers tried to observe the relation between the microstructure properties and the mechanical characteristics of duplex stainless steel alloys, but they did not establish an exact relation. In fact, a very complex and complicated relationship is governing the link between the microstructural properties that the exhibited mechanical behaviour. Moreover, nearly all microstructural properties directly affect each other. For instance, the grain size of the ferrite phase (δ) affects the grain size of the austenite phase (γ), the width of the ferrite/austenite boundaries and, many other properties. Because of the complex and the complicated relationship between the microstructural properties and the exhibited mechanical behaviour, is nearly impossible to assess how a change in a single microstructural characteristic is influencing a single mechanical property. Also, one must take into consideration that the material's microstructure is easily influenced by the applied thermomechanical processing route and, therefore, many processing parameters can be

considered of extreme importance and must be accounted. A first step in gaining insight into this complex equation is to completely characterize the processed material, from the microstructural and the mechanical point of view, by qualitative and quantitative advanced techniques. A second step consists of correlations establishments between the accounted parameters followed by the quantification of this link/relation.

Considering the specific case of super duplex stainless steel alloys, several modern mechanical processing operations, such as rolling, forging, extrusion, etc, can be employed to apply a certain plastic strain. Also, several thermal processing operations, such as annealing, quenching, tempering, ageing, etc, can be employed. All being able to induce changes in the alloy's microstructure and, therefore, changes in the alloy's mechanical behaviour.

4.2. Research questions and hypothesis

In industrial components/parts, manufactured from the super duplex stainless steel (SDSS) alloys, failure occurred, speciality, when these parts were working in harsh conditions, consisting of high temperatures and chloride-rich environments, by stress corrosion cracking and/or pitting/crevice corrosion. Therefore, choosing a suitable alloy in these fields could potentially take an important role in the extension of life by increasing the alloy's corrosion resistance and, also, its mechanical properties.

Usually, the SDSS alloys can be used in many corrosive environments within the temperature range of -50ºC to less than 300ºC. *So, if we could increase the alloy's ability to resist chloride corrosion and, also, increase its mechanical properties by applying a proper thermomechanical processing cycle, can lead to a big impact in expanding the utilization of the SDSS alloys.* The temperature at which the mechanical processing is performed and the temperature of the applied thermal processing, as well as, its duration can have a big impact on the final microstructural and mechanical characteristics of the processed SDSS alloy.

As investigated material, the super duplex stainless steel (SDSS) S32760 / F55 alloy was considered, due to its promising utilization in many industrial fields, from the oil/gas industry to the desalination.

4.3. Main objectives of the thesis

The thesis objectives are categorized as follows:

- to have a better understanding of how to adequately process the S32760 / F55 SDSS alloy, using various processing parameters and to quantify the induced effects on the alloy's microstructure and its mechanical behaviour;
- to optimize the final microstructural and mechanical characteristics of the S32760 / F55 SDSS alloys;
- to employ various techniques of investigation, such as scanning electron microscopy (SEM) and X-ray diffraction (XRD) for the microstructural properties and tensile and microhardness testing for the mechanical characteristics.

4.4. Structure of the thesis

The thesis structure consists of two parts. The first part contains the overview and introduction presented in chapter 1, the metallurgical view of stainless steels and their applications in chapter 2, while chapter 3 presents a general overview of the mechanical and thermal processing operation. The second part contains the experimental section, starting with the problem statement and the objective of the thesis in chapter 4, the methodology of

samples processing and advanced characterization in chapter 5, microstructural evolution during thermomechanical processing presented in chapter 6, mechanical properties evolution during thermomechanical processing presented in chapter 7 and, general conclusions, personal contributions, recommendations, and future research directions presented in chapter 8.

The thesis finishes with the list of references, appendices and the list of publications/results dissemination.

Chapter 5: methodology

5.1 Introduction

This chapter presents a detailed description of the alloy sampling system, the utilized equipment and the applied characterization methods.

5.3. Thermomechanical processing routes applied to UNS S32760/F55 SDSS

Four experiments performed with a UNS S32760/F55 SDSS alloy. Initial dimensions of thermo-mechanically processed samples are 100 mm length, 14.8 mm width and 7.5 mm thickness. Four different temperatures of hot rolling were used in the experiments (1000, 1050, 1100, 1150)ºC, all heat treatments carried out using a high temperature NABERTHERM furnace.

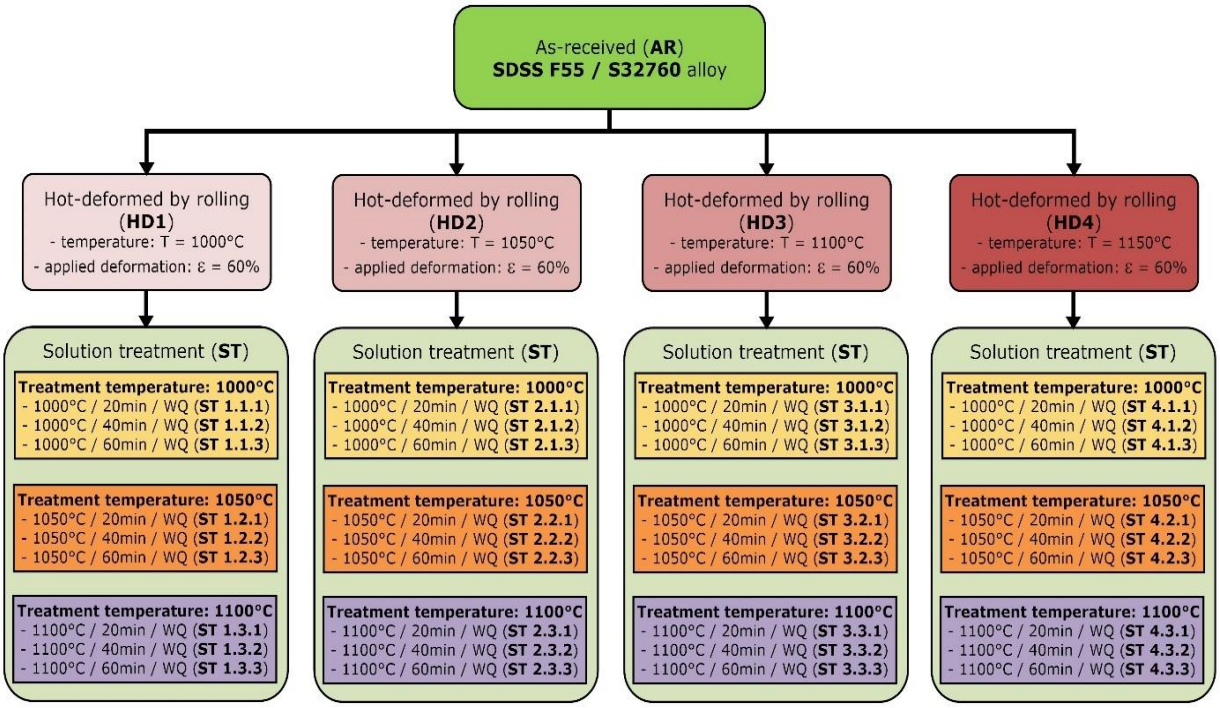

Fig. 5.1 *Schematic representation of the experiments of thermomechanical processing applied SDSS F55 alloy*

After removing the samples from the furnace, the samples were subjected to the hot deformation (HD) by rolling, using a ∅180 x 150 mm duo rolling-mill. The thickness of samples subjected to hot deformation decreased during deformation. Each hot deformation processing stage was followed by a solution treatment, using different treatment temperatures (1000°C, 1050°C and 1100ºC) and different treatment durations (20min, 40min and 60min), as shown in Figure 5.1.

5.4 Metallographic analysis

Specimens were removed from all processed samples for metallographic investigation. All specimens were prepared with excellent surface finish and, were hot mounted in a cylindrical sampler of PHENOCURE black phenolic conductive resin using a BUEHLER Simplimet hydraulic mounting press. The operation allows users to control the mounting cycle. All specimens were, also, subjected to mechanical grinding with SiC paper from (180–1200) grit, in six passes (60s/pass) and polishing by 6μm and 1μm polycrystalline diamond suspension (180s/pass) using a Metkon DIGIPREP Accura.

All specimens were polished in high quality 0.05μm colloidal silica suspension mixed within a 1/5 ratio of 20% H_2O_2 (300s/step) and finally vibratory polishing within 0.02μm colloidal silica mixed within a 1/5 ratio of 20% H_2O_2 (3.6ks) using a BUEHLER Vibromet 2. The VibroMet2 polishing machine assures chemo-mechanically polishing for sample surface finishing and fits for electron-backscatter diffraction (EBSD) examination.

The microstructural characterization was performed using a Scanning Electron Microscopy (SEM) - TESCAN VEGA II – XMU. The dispersion of alloying elements within the S32760 / F55 SDSS alloy microstructure was determined by Energy Dispersive Spectroscopy (EDS) using a BRUKER x-Flash 6/30 EDS detector connected with the TESCAN VEGA II – XMU SEM. The EBSD characterization was performed using a BRUKER e-Flash 1000 EBSD detector connected with the TESCAN VEGA II – XMU SEM.

The alloy's microstructure analysis was completed with X-ray diffraction (XRD) investigations. The XRD investigations were performed using a Rigaku Mini-Flex 600 diffractometer. The XRD investigations allowed rapid phase identification and phase characteristics for as-received specimens.

5.5. Mechanical analysis

The mechanical properties of all specimens were investigated in the rolling direction (RD) - transverse direction (TD) samples plane. The tensile strength test was performed at room temperature by using an INSTRON 3382universal machine. All investigated specimens were prepared for tensile testing and machined with a "dog-bone" shape. The average values of ultimate tensile strength (σ_{UTS}), 0.2% yield strength ($\sigma_{0.2\%}$) and fracture elongation (ε_f) were estimated to study the correlation between microstructure and mechanical behaviour. Vickers microhardness testing was performed at room temperature using INNOVATEST Falcon 500 equipment. The load applied to the specimens during microhardness testing was 0.1kg (0.98066 N) with a dwell time of 10s for the ferrite and austenite phases, while for the sigma phase the load was 0.025kg (0.24516 N).

Chapter 6: Microstructural properties evolution during thermomechanical processing of F55 SDSS alloy

6.1. Introduction

This chapter is focused on the advanced analysis of the microstructural evolution during thermomechanical processing by hot-deformation and different solution treatments of F55 (UNS S32760) super duplex stainless steel (SDSS) alloy (see Fig. 6.1).

As observed (see Fig. 6.1), the applied thermomechanical processing route assumes, firstly, a hot-deformation (at different temperatures: 1000°C; 1050°C; 1100°C; 1150°C) and, secondly, a solution treatment (at different temperatures: 1000°C; 1050°C; 1100°C; and different treatment durations: 20min; 40min; 60min). By applying such a processing route

one can investigate the evolution of the F55 alloy's microstructure in the complex space of thermomechanical processing conditions, which can offer important observations/clues in understanding the microstructural evolution during thermomechanical processing.

The microstructural characterization can be performed using the following investigation techniques: XRD (X-ray Diffraction), SEM-EBSD (Scanning Electron Microscopy–Electron Backscattering Diffraction), SEM-EDS (SEM–Energy Dispersive Spectroscopy), SEM-SE (SEM–Secondary Electrons), SEM-BSE (SEM–Backscattered Electrons), etc. Based on these investigation techniques, it can obtain important data concerning the nature and structure, volume fraction, grain size and chemistry of the constituent phases.

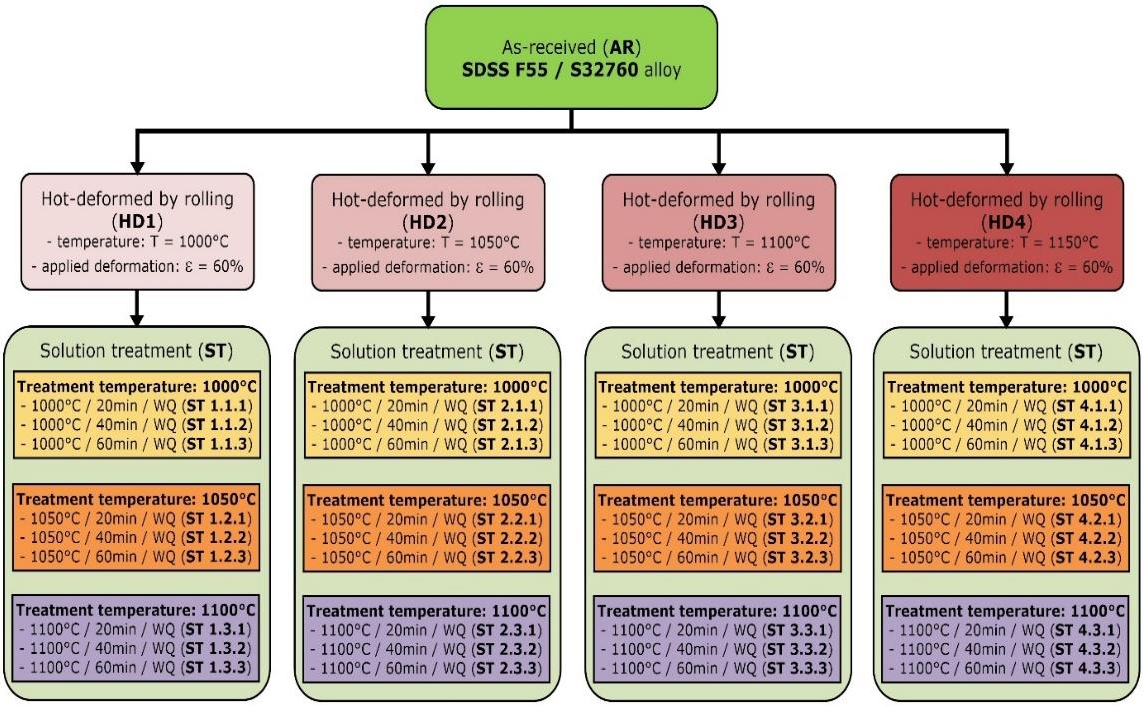

Fig. 5.1 *Thermomechanical processing scheme applied to F55 (UNS S32760) SDSS alloy.*

6.2. As-received (AR) state

The as-received (AR) F55 (UNS S32760) SDSS alloy was completely characterized from the microstructural and mechanical point of view. The microstructural characterization employed XRD, SEM-EBSD and SEM-EDS investigation techniques.

By XRD analysis (see Fig. 6.2) the following phases were identified:

- ***ferrite phase*** (***δ***): indexed in 229 (Im-3m) body centred cubic (BCC) crystalline system, with a lattice parameter a = 2.883Å, for which the following diffraction peaks were observed: (110) - 44.41°; (200) - 64.59°; (211) - 81.76°.
- ***austenite phase*** (***γ***): indexed in 225 (Fm-3m) face centred cubic (FCC) crystalline system, with a lattice parameter a = 3.616Å, for which the following diffraction peaks were observed: (111) - 43.31°; (200) - 50.44°; (220) - 74.14°.

Table 6.1

Average volume fraction [%wt] and average grain size [μm] for AR F55 SDSS alloy.

Structural state	Average volume fraction [%wt]			Average grain-size [μm]		
	$\gamma + \gamma_2$	δ	σ	$\gamma + \gamma_2$	δ	σ
As-received **(AR)** sample	50±0.7	49±0.3	-	88±3	127±6	-

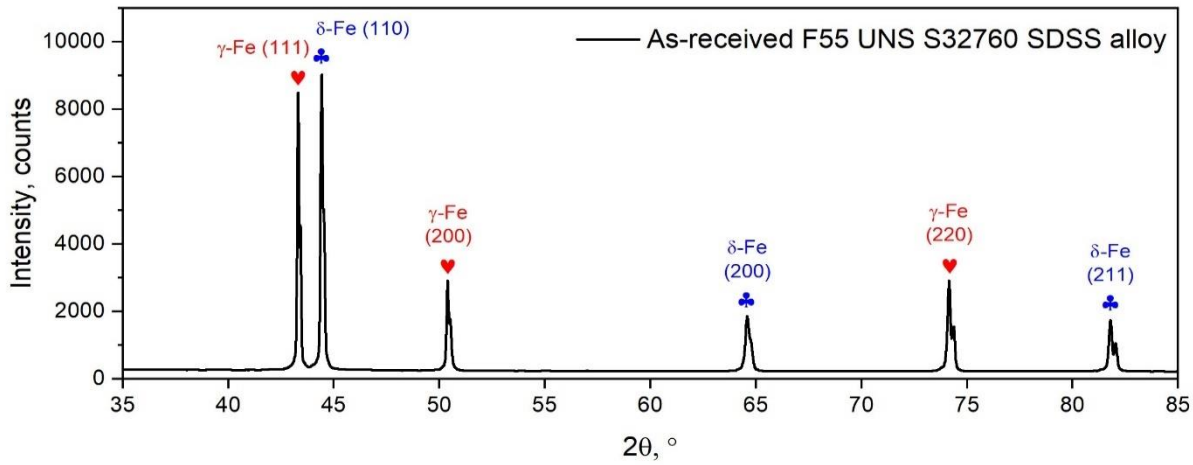

Fig. 6.2 *XRD spectra of as-received (AR) F55 (UNS S32760) SDSS alloy.*

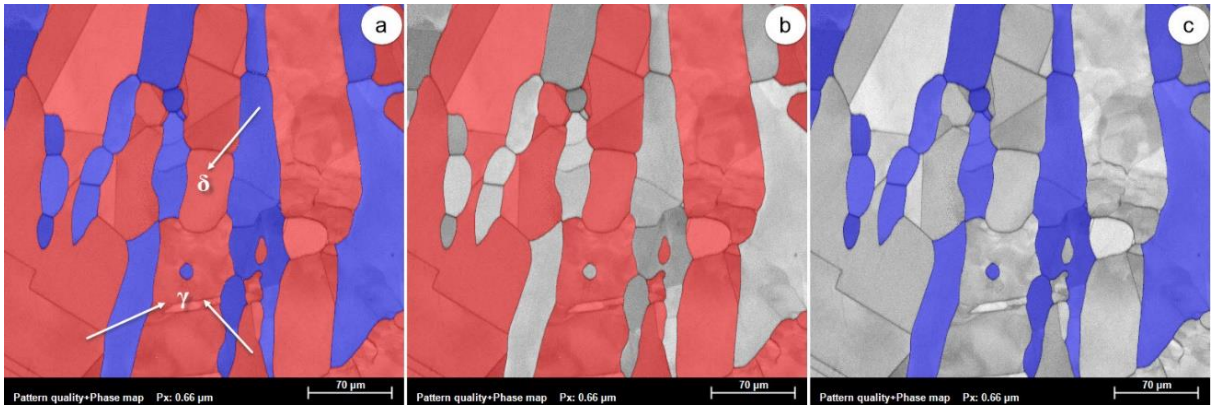

Fig. 6.3. *SEM-EBSD microstructure analysis of as-received alloy; distribution of ferrite and austenite phases (a), austenite phase distribution (b), ferrite phase distribution (c).*

The SEM-EBSD analysis (see Fig. 6.3) showed that the AR F55 SDSS alloy consists of approximatively equal volume fractions (50±0.7 / 49±0.3) of γ- phase / δ-phase (see Table 6.1). It can observe that the γ-phase shows an island-like morphology in the δ-phase matrix. Also, can be observed that the average grain-size of the γ- phase is close to 88±3 µm while the δ-phase is close to 127±6 µm (see Table 5.1). The SEM-EDS analysis of alloying elements distribution maps for Fe, Cr, Ni, Mo, Al, Si, Mn and Cu (see Fig. 6.4b – 6.4i) show that the ferrite (δ-phase) is enriched in Cr, Mo, W and Si and depleted in Ni, Mn and Cu, while the austenite (γ-phase) is enriched in Ni, Mn and Cu and depleted in Cr, Mo, W and Si. These qualitative observations are supported by the computed chemical compositions of both γ-phase and δ-phase, which are presented in Tables 6.3 and 6.4. Figure 6.4a shows a characteristic SEM-BSE image of AR F55 SDSS alloy, in which it can easily identify the ferrite (coloured in light grey) and austenite (coloured in dark grey) constituent phases. The overall/global chemical composition of AR F55 SDSS alloy is presented in Table 6.2, in which it can be observed that the composition falls within the prescription for the 1.4501 / UNS S32760 / F55 alloy [101].

The SEM-EDS analysis shows that the main γ-stabilizing alloying element is constituted by Ni, which must be in a higher weight fraction in order to surpass its solubility limit in the δ-phase. In the AR F55 SDSS alloy the Ni weight fraction in the matrix δ-phase is close to 5.54 (%wt), while in the γ-phase being close to 8.69 (%wt) and an overall average close to 7.50 (%wt).

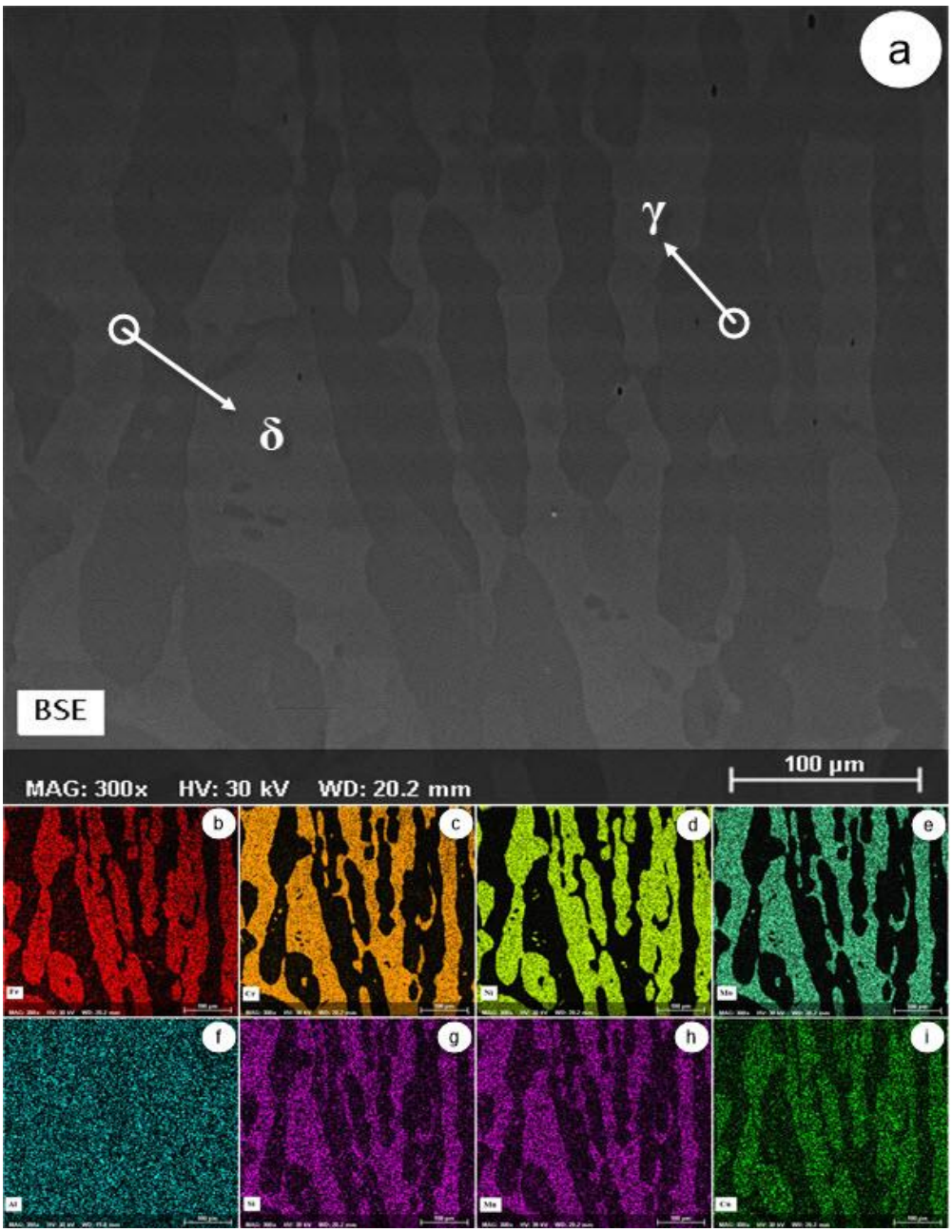

Fig. 6.4. *SEM-BSE microstructural image of AR F55 SDSS alloy (a); SEM-EDS images of distribution map for Fe (b); Cr (c); Ni (d); Mo (e); Al (f); Si (g); Mn (h); Cu (i).*

Table 6.2

Chemical composition of AR F55 SDSS alloy[101].

Elem. At.	No.	Mass norm. %	Atom abs %	Error % (1 Sigma)	Rel. error % (1 Sigma)
Iron	26	60.19	58.67	1.62	2.56
Chromium	24	25.85	27.06	0.73	2.7
Nickel	28	7.50	6.95	0.22	2.78
Molybdenum	42	2.78	1.58	0.10	3.54
Aluminum	13	1.45	2.93	0.10	6.64
Silicon	14	0.86	1.67	0.07	7.21
Manganese	25	0.60	0.59	0.04	6.53
Copper	29	0.58	0.50	0.04	6.55
Tungsten	74	0.20	0.06	0.03	14.45
		100%	100%		

Table 6.3

Chemical composition for the austenite (γ-phase)[101].

Elem. At.	No.	Mass norm. %	Atom abs %	Error % (1 Sigma)	Rel. error % (1 Sigma)
Fe	26	62.58	61.85	1.55	2.57
Cr	24	25.72	27.30	0.68	2.72
Ni	28	8.69	8.18	0.24	2.83
Mo	42	1.33	0.76	0.11	8.35
W	74	0.03	0.01	0.00	11.83
Si	14	0.34	0.67	0.04	13.23
Mn	25	0.55	0.55	0.04	7.89
Cu	29	0.59	0.51	0.04	7.78
V	23	0.166	0.17	0.03	20.73
		100.00	100.00		

Table 6.4

Chemical composition for the ferrite (δ-phase)[101].

Elem. At.	No.	Mass norm. %	Atom abs %	Error % (1 Sigma)	Rel. error % (1 Sigma)
Fe	26	60.77	60.41	1.53	2.57
Cr	24	28.50	30.43	0.76	2.71
Ni	28	5.54	5.24	0.16	3.04
Mo	42	3.23	1.87	0.17	5.53
W	74	0.43	0.13	0.04	10.08
Si	14	0.45	0.89	0.05	11.06
Mn	25	0.46	0.46	0.04	8.82
Cu	29	0.47	0.41	0.04	9.01
V	23	0.14	0.16	0.03	21.88
		100.00	100.00		

6.3. Hot deformation at 1000ºC (HD1) state

The microstructural SEM-EBSD analysis of hot deformed, by rolling, at 1000°C (HD1) state is presented in Figure 6.5. It can be noticed that the applied intense (total applied deformation degree = 60%) hot deformation leads to the following observations, firstly, it can observe that a new phase (see Fig. 6.5a - coloured in yellow) is generated/precipitated within the microstructure, this new phase was identified as the σ-phase and, secondly, both initial δ and γ phases are showing signs of intense deformation.

Table 6.5

Average volume fraction [%wt] and average grain size [μm] for HD1 state.

Structural state	Average volume fraction [%wt]			Average grain-size [μm]		
	γ + γ2	**δ**	**σ**	**γ + γ2**	**δ**	**σ**
Hot deformed at 1000°C (**HR1**)	50.7	45.8	3.5	19.3	57.5	5.32

In depth analysis of σ-phase precipitation shows that, mainly, the σ-phase precipitation occurred at δ to γ phase boundaries, within δ-phase, in sites where favourable conditions are occurring to promote a δ → σ precipitation reaction. Also, in some small areas, it can observe that the σ-phase precipitation occurred at δ to δ phase boundaries, within δ-phase, in sites where favourable conditions are occurring to promote a δ → σ + γ_2 eutectoid precipitation reaction. The analysis of variations in the average volume fraction of constituent phases

shows that during hot deformation (at 1000°C) only in the case of δ-phase and σ-phase are recorded variations, confirming that the γ-phase does not contribute to σ-phase precipitation (see Table 6.4). The overall observed σ-phase weight fraction was situated close to 3.5 (%wt), while the average grain-size was situated close to 5.32μm (see Table 6.5).

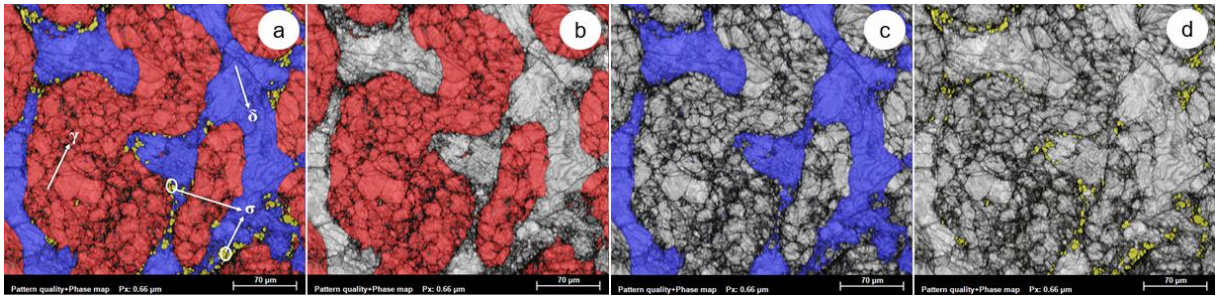

Fig. 6.5. *SEM-EBSD microstructure of hot-rolled at 1000ºC (HD1) state (a); austenite phase (b); ferrite phase (c); sigma phase (d).*

In terms of mechanical behaviour, the occurrence of σ-phase is an undesirable phase, due to its deleterious effect - induced embrittlement – on alloy's toughness properties [102].

Morphological aspects of deformed δ and γ phases show the presence of intense deformed and fragmented grains also, the presence of strain-hardening phenomena within the microstructure. Comparing the δ-phase grains with the γ-phase grains, it can observe that the γ-phase grains are showing signs of more intense fragmentation in comparison with the δ-phase grains, while δ-phase grains are showing signs of more intense strain-hardening in comparison with the γ-phase grains. These observations can be explained based on differences in the crystallography of both phases, which assumes that the FCC crystalline system (γ-phase) is accommodating the applied deformation better compared to the BCC crystalline system (δ-phase) by slip/twinning for the same applied stress/strain level, due to it's easier to activate slip/twinning on its higher atomic density planes [103] also, leading to a lower internal defect density (related to the strain-hardening) resulted after accommodating the applied stress/strain [104]. The computed average grain-size of both δ-phase and γ-phase shows that the fragmentation of the γ-phase grains is much more intense when compared to δ-phase grains, it can observe that the average grain-size of the γ-phase was situated close to 19.3μm, while in the δ-phase case close to 57.5μm (see Table 6.5).

6.4. Solution treatment at 1000°C (ST1) state

6.4.1. Solution treatment at 1000°C (ST1.1) state

Figure 6.6 shows the microstructural evolution as a result of applying a solution treatment at 1000°C, with a treatment duration of 20min (Figure 6.6a), 40min (Figure 6.6b) and 60min (Figure 6.6c). In the case of the solution treatment performed with a treatment duration of 20min (ST 1.1.1) it can observe that the initially intensely deformed δ-phase and γ-phase grains are fully recrystallized, all grains showing uniform morphology and a very low defect density. The average grain-size of the γ-phase is close to 15.1μm while, the δ-phase is close to 51.8μm. Besides the δ-phase and γ-phase it can observe that the σ-phase is present in the microstructure, suggesting that the treatment duration is still low enough to assure precipitation of the σ-phase (Figure 6.6a). Analysing the location of σ-phase precipitates it can observe that, mainly, the precipitation occurred at δ to γ phase boundaries, within δ-phase, in sites where favourable conditions are met in order to promote a δ → σ precipitation. Also, it can be seen in the sites at δ to δ phase boundaries, within δ-phase, where favourable

conditions are met in order to promote δ → σ + γ_2 eutectoid precipitation/decomposition. The overall observed σ-phase weight fraction was situated close to 2.7 (%wt), while the average grain-size was situated close to 4.9μm (see Table 6.6). The analysis of variations in the average volume fraction of constituent phases shows that during solution treatment (at 1000°C with a treatment duration of 20min) only in the case of δ-phase and σ-phase are recorded significant variations, confirming that the σ-phase is linked to the δ-phase and not linked to the γ-phase (see Table 6.6).

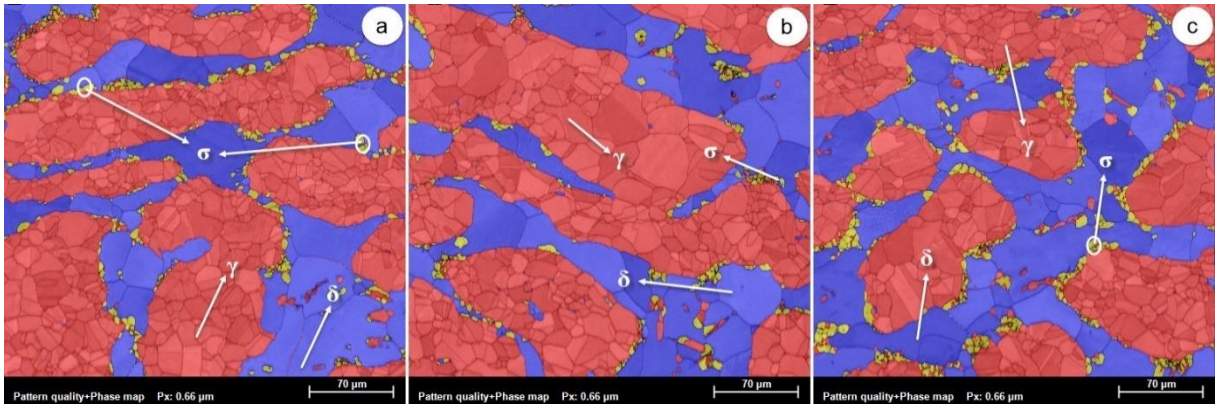

Fig. 6.6. *Characteristic SEM-EBSD microstructural images of solution treated samples at 1000°C (ST 1.1) state, with a treatment duration of 20min (ST 1.1.1) (a); 40min (ST 1.1.2) (b); 60min (ST 1.1.3) (c).*

Increasing the treatment duration to 40min (Figure 6.6b) it can be seen that the weight fraction of the σ-phase is increasing, being recorded close to 3.7 (%wt). It can be noticed that the σ-phase precipitates are located, almost in equal fractions, at δ to γ and δ to δ phase boundaries, suggesting that with treatment duration increment the precipitation mechanism is shifted towards δ → σ + γ_2 eutectoid precipitation/decomposition, an observation confirmed by the small increase observed in the (γ + γ_2) weight fraction, form 50.3(%wt) to 51.6(%wt) (see Table 6.6). In terms of average grain-size it can observe an increase for all phases, from 15.1μm to 19.6μm for γ-phase, from 51.8μm to 54.9μm for δ-phase and from 4.9μm to 5.5μm for σ-phase, due to the grain-growth by diffusion mechanism (see Table 6.6).

Table 5.6

Average volume fraction [%wt] and average grain size [μm] for ST 1.1 state.

Structural state / Solution treatment at 1000ºC (ST 1.1)	**Average volume fraction [%wt]**			**Average grain-size [μm]**		
	γ + γ_2	**δ**	**σ**	**γ + γ_2**	**δ**	**σ**
Solution treated: 1000°C/20mins/WQ (**ST 1.1.1**)	50.3	47.0	2.7	15.1	51.8	4.9
Solution treated: 1000°C/40mins/WQ (**ST 1.1.2**)	51.6	44.9	3.5	19.6	54.9	5.5
Solution treated: 1000°C/60mins/WQ (**ST 1.1.3**)	51.9	42.6	5.5	16.6	57.7	6.0

By increasing the treatment duration to 60min (Figure 6.6c), the weight fraction of the σ-phase is still increasing, reaching a value close to 5.5 (%wt). It can be seen that the σ-phase precipitates are located, mainly, at δ to δ phase boundaries, within δ-phase, where favourable conditions are meet in order to promote δ → σ + γ_2 eutectoid precipitation / decomposition, suggesting that the δ → σ + γ_2 eutectoid precipitation / decomposition tends to become the most influential σ-phase precipitation mechanism, observation confirmed by further observed increase in the (γ + γ_2) weight fraction, form 51.6(%wt) to 51.9(%wt) (see Table 5.6). In terms of average grain-size, it can observe that both the δ-phase and the σ-phase show an increase to 57.7μm and, respectively, 6μm, while the γ-phase shows a decrease to 16.6μm. Must be noticed that this is an apparent decrease, due to the increasing number of newly

precipitated γ_2-phase small-size grains generated within the δ-phase by the eutectoid decomposition.

6.4.2. Solution treatment at 1050°C (ST1.2) state

Figure 6.7 shows the microstructural aspects obtained after applying a solution treatment at 1050°C, with a treatment duration of 20min (Figure 6.7a), 40min (Figure 6.7b) and 60min (Figure 6.7c).

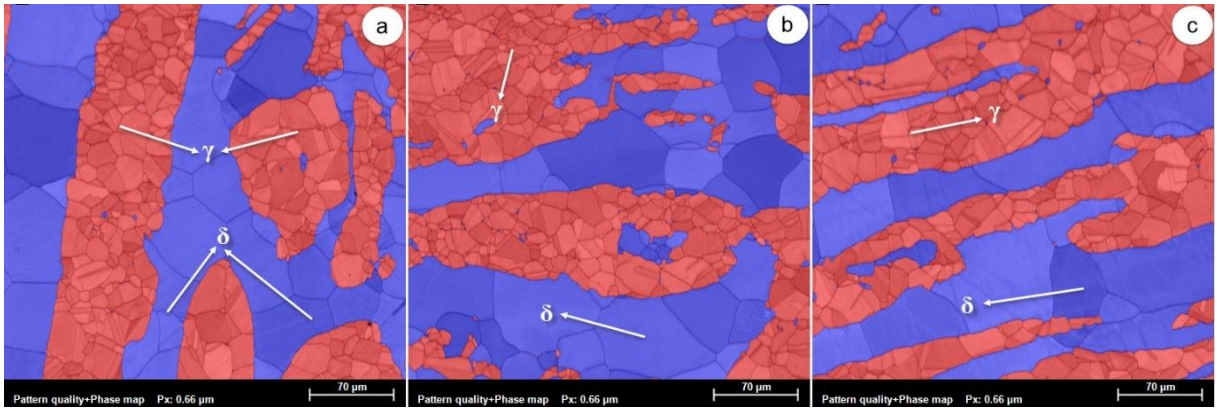

Fig. 6.7. *Characteristic SEM-EBSD microstructural images of solution treated samples at 1050°C (ST 1.2) state, with a treatment duration of 20min (ST 1.2.1) (a); 40min (ST 1.2.2) (b); 60min (ST 1.2.3) (c).*

In the case of the solution treatment performed with a treatment duration of 20min (ST 1.2.1) it can observe that the initially intensely deformed δ-phase and γ-phase grains are fully recrystallized, all grains showing uniform morphology and a very low defect density (see Figure 6.7a). The average grain-size of the γ-phase is close to 15.8µm while, the δ-phase is close to 52.8µm (see Table 6.7). No other precipitated secondary phases are observed, suggesting that the treatment temperature is situated above the threshold temperature to induce precipitation of the deleterious σ-phase. The overall average weight fraction of the observed γ-phase was situated close to 51.5 (%wt), while the average weight fraction of the δ-phase was close to 48.5 (%wt) (see Table 6.7). Increasing the treatment duration to 40min (Figure 6.7b) results in a small increase in the weight fraction of the δ-phase, from 48.5 (%wt) to 49.5 (%wt), suggesting that at this treatment duration the γ → δ phase transition is occurring, but with a small transformation rate. Also, it can be seen that the average grain-size of the constituent γ-phase and δ-phase are increasing, from 15.8µm to 18.4µm and, respectively, from 52.8µm to 55.1µm, due to the grain-growth by diffusion mechanism (see Figure 6.7b and Table 6.7).

Table 6.7

Average volume fraction [%wt] and average grain size [µm] for ST 1.2 state.

Structural state / Solution treatment at 1050°C (ST 1.2)	**Average volume fraction [%wt]**			**Average grain-size [µm]**		
	γ + γ₂	**δ**	**σ**	**γ + γ₂**	**δ**	**σ**
Solution treated: 1050°C/20mins/WQ (**ST 1.2.1**)	51.5	48.5	-	15.8	52.8	-
Solution treated: 1050°C/40mins/WQ (**ST 1.2.2**)	50.5	49.5	-	18.4	55.1	-
Solution treated: 1050°C/60mins/WQ (**ST 1.2.3**)	49.2	50.8	-	20.1	58.5	-

Further increasing the treatment duration to 60min (Figure 6.7c) leads to a continuous increase in the weight fraction of the δ-phase, reaching 50.8 (%wt), confirming that at 1050°C and long enough durations the γ → δ phase transition is occurring and can be

significant in terms of transformed weight fraction (see Figure 6.9c and Table 6.7). Also, the noticed increase in the average grain-size of both constituent γ-phase and δ-phase, to 20.1μm and, respectively, to 58.5μm, is confirming that the grains are growing due to the diffusion mechanism (see Figure 6.7c and Table 6.7).

6.4.3. Solution treatment at 1100°C (ST1.3) state

Figure 6.8 shows the microstructural aspects obtained after applying a solution treatment at 1100°C, with a treatment duration of 20min (Figure 6.8a), 40min (Figure 6.8b) and 60min (Figure 6.8c). In the case of the solution treatment performed with a treatment duration of 20min (ST 1.3.1) it can be observed that the microstructure consists of fully recrystallized constituent γ-phase and δ-phase grains, all grains showing uniform morphology and a very low defect density. The average grain-size of the γ-phase is close to 19.4μm while, the δ-phase is close to 56μm (see Figure 6.8a and Table 6.8). No other precipitated secondary phases are observed. The overall average weight fraction of the observed γ-phase was situated close to 48.3 (%wt), while the average weight fraction of the δ-phase was close to 51.7 (%wt) (see Table 6.8).

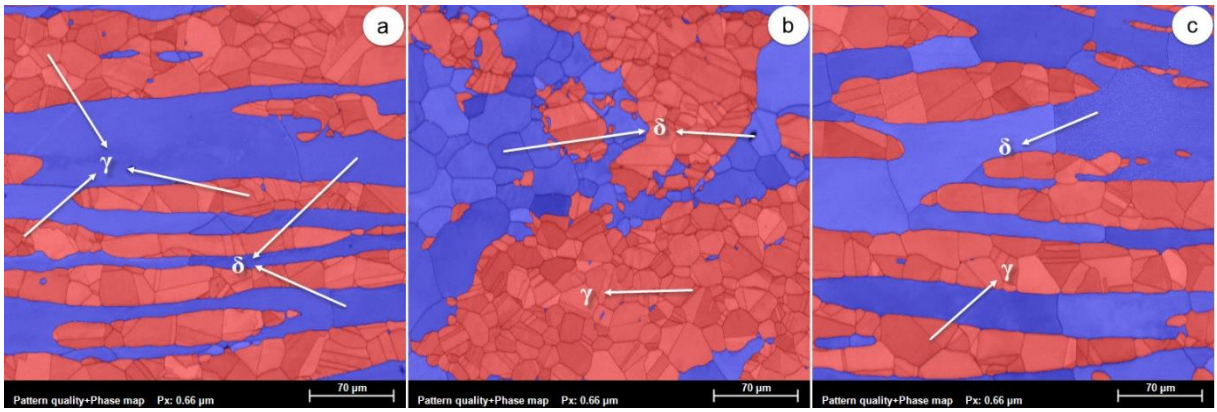

Fig. 6.8. *Characteristic SEM-EBSD microstructural images of solution treated samples at 1100°C (ST 1.3) state, with a treatment duration of 20min (ST 1.3.1) (a); 40min (ST 1.3.2) (b); 60min (ST 1.3.3) (c).*

Increasing the treatment duration to 40min (ST 1.3.2) (Figure 6.8b) results in an increase in the weight fraction of the δ-phase, from 51.7 (%wt) to 53.6 (%wt), suggesting that at this treatment duration the γ → δ phase transition is occurring, but with a higher transformation rate comparing with the solution treatment performed at 1050°C (ST 1.2) case. Also, it can be noticed that the average grain-size of the constituent γ-phase and δ-phase are increasing, to 22.6μm and, respectively, to 78.2μm, indicting, also, that the grain-growth rate is higher compared with the solution treatment performed at 1050°C (ST 1.2) case (see Figure 6.8b and Table 6.8).

Table 6.8

Average volume fraction [%wt] and average grain size [μm] for ST 1.3 state.

Structural state / Solution treatment at 1100°C (ST 1.3)	**Average volume fraction [%wt]**			**Average grain-size [μm]**		
	γ + γ2	**δ**	**σ**	**γ + γ2**	**δ**	**σ**
Solution treated: 1100°C/20mins/WQ (**ST 1.3.1**)	48.3	51.7	-	19.4	56.0	-
Solution treated: 1100°C/40mins/WQ (**ST 1.3.2**)	46.4	53.6	-	22.6	78.2	-
Solution treated: 1100°C/60mins/WQ (**ST 1.3.3**)	44.9	55.1	-	26.5	88.3	-

Further increasing the treatment duration to 60min (ST 1.3.3) (Figure 6.8c) leads to a continuous increase in the weight fraction of the δ-phase, reaching 55.1 (%wt), confirming

that at 1100°C and long enough durations the γ → δ phase transition is occurring and is significant in terms of transformed weight fraction (see Figure 6.8c and Table 6.8). Also, it can notice a significant increase in the average grain-size of both constituents γ-phase and δ-phase, to 26.5μm and, respectively, 88.6μm (see Figure 6.8c and Table 6.8).

6.5. Hot deformation at 1050ºC (HD2) state

The microstructural SEM-EBSD analysis of hot deformed, by rolling, at 1050°C (HD2) state is presented in Figure 6.13. It can be observed that the applied intense (total applied deformation degree = 60%) hot deformation leads to the following observations, firstly, it can be seen that σ-phase generated/precipitated in continue within the microstructure (see Fig. 6.9a - coloured in yellow) is generated/precipitated within the microstructure and, secondly, both initial δ and γ phases are showing signs of intense deformation.

Table 6.9

Average volume fraction [%wt] and average grain size [μm] for HD2 state.

Structural state	Average volume fraction [%wt]			Average grain-size [μm]		
	$\gamma + \gamma_2$	δ	σ	$\gamma + \gamma_2$	δ	σ
Hot deformed at 1050°C (**HR2**)	48.8	50.8	0.4	33.2	77.2	5.32

In-depth analysis of σ-phase precipitation shows that, mainly, the σ-phase precipitation occurred at δ to γ phase boundaries, in sites where favourable conditions are occurring to promote a δ → σ precipitation reaction. The analysis of variations in the average volume fraction of constituent phases shows that during hot deformation (at 1050°C) only in the case of δ-phase and σ-phase did not record big variations, confirming that the γ-phase contributes to σ-phase precipitation (see Table 6.9). The overall observed σ-phase weight fraction was situated close to 0.4 (%wt), while the average grain-size was situated close to 5.32μm (see Table 6.9).

Morphological aspects of deformed δ and γ phases show the presence of intense deformed and fragmented grains also, the presence of strain-hardening phenomena within the microstructure. Comparing the δ-phase grains with the γ-phase grains, it can be noticed that the γ-phase grains are showing signs of more intense fragmentation in comparison with the δ-phase grains, while δ-phase grains are showing signs of more intense strain-hardening in comparison with the γ-phase grains. The computed average grain-size of both δ-phase and γ-phase shows that the fragmentation of the γ-phase grains is much more intense when compared to δ-phase grains, it can observe that the average grain-size of the γ-phase was situated close to 33.2 μm, while in the δ-phase case close to 77.2 μm (see Table 6.9).

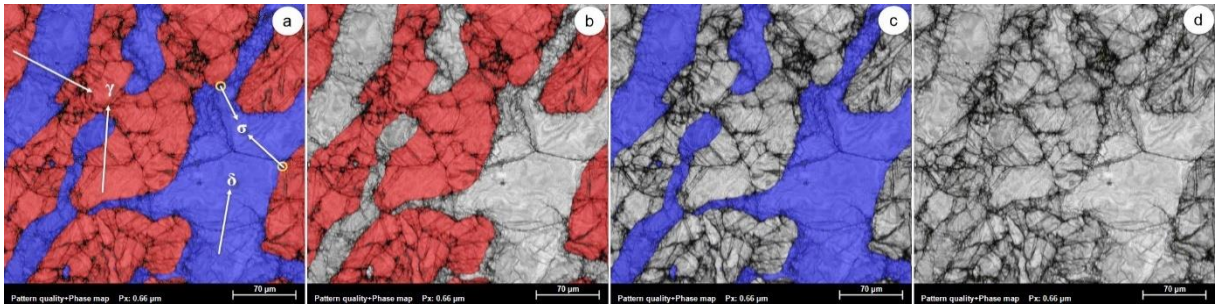

Fig. 6.9. *SEM-EBSD microstructure of hot-rolled at 1050ºC (HD2) state (a); austenite phase (b); ferrite phase (c); sigma phase (d).*

6.6. Solution treatment at 1050°C (ST2) state

6.6.1. Solution treatment at 1000°C (ST2.1) state

Figure 6.10 shows the microstructural evolution as a result of applying a solution treatment at 1000°C, with a treatment duration of 20min (Figure 6.10a), 40min (Figure 6.10b) and 60min (Figure 6.10c). In the case of the solution treatment performed with a treatment duration of 20min (ST 2.1.1), it may be observed that the initially intensely deformed δ-phase and γ-phase grains are fully recrystallized, all grains showing uniform morphology and a very low defect density. The average grain-size of the γ-phase is close to 19.1μm while, the δ-phase is close to 57.2μm. Besides the δ-phase and γ-phase it can observe that the σ-phase is present in the microstructure, suggesting that the treatment duration is still low enough to assure precipitation of the σ-phase (Figure 6.10a). Analysing the location of σ-phase precipitates it can be observed that, mainly, the precipitation occurred at δ to γ phase boundaries, within δ-phase, in sites where favourable conditions are met in order to promote a δ → σ precipitation. Also, it may be seen sites at δ to δ phase boundaries, within δ-phase, where favourable conditions are met in order to promote δ → σ + γ_2 eutectoid precipitation/decomposition. The overall observed σ-phase weight fraction was situated close to 1.1 (%wt), while the average grain-size was situated close to 5.3μm (see Table 6.10).

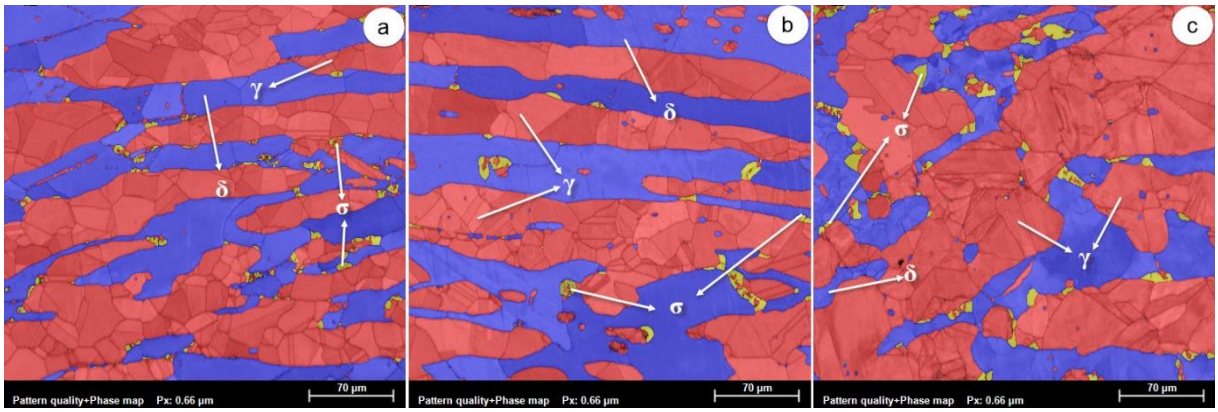

Fig. 6.10. *Characteristic SEM-EBSD microstructural images of solution treated samples at 1000°C (ST 2.1) state, with a treatment duration of 20min (ST 2.1.1) (a); 40min (ST 2.1.2) (b); 60min (ST 2.1.3) (c).*

The analysis of variations in the average volume fraction of constituent phases shows that during solution treatment (at 1000°C with a treatment duration of 20min) only in the case of δ-phase and σ-phase are recorded significant variations, confirming that the σ-phase is linked to the δ-phase and not linked to the γ-phase (see Table 6.10).

Table 6.10

Average volume fraction [%wt] and average grain size [μm] for ST 2.1 state.

Structural state / Solution treatment at 1000ºC (ST 1.1)	**Average volume fraction [%wt]**			**Average grain-size [μm]**		
	γ + γ_2	**δ**	**σ**	**γ + γ_2**	**δ**	**σ**
Solution treated: 1000°C/20mins/WQ (**ST 2.1.1**)	50.2	48.7	1.1	19.1	57.2	5.3
Solution treated: 1000°C/40mins/WQ (**ST 2.1.2**)	51.7	46.6	1.7	24.4	69.2	7.2
Solution treated: 1000°C/60mins/WQ (**ST 2.1.3**)	52.6	44.5	2.9	29.5	74.5	8.2

Increasing the treatment duration to 40min (Figure 6.10b) it can be seen that the weight fraction of the σ-phase is increasing, being recorded close to 1.7 (%wt). It can be noticed that the σ-phase precipitates are located, almost in equal fractions, at δ to γ and δ to δ phase boundaries, suggesting that with treatment duration increment the precipitation mechanism is shifted towards δ → σ + γ_2 eutectoid precipitation/decomposition, an observation confirmed

by the small increase observed in the ($\gamma + \gamma_2$) weight fraction, form 50.2(%wt) to 51.7(%wt) (see Table 6.10). In terms of average grain-size it can observe an increase for all phases, from 19.1μm to 24.4μm for γ-phase, from 57.2μm to 69.2μm for δ-phase and from 5.3μm to 7.2μm for σ-phase, due to the grain-growth by diffusion mechanism (see Table 6.10).

Increasing the treatment duration to 60min (Figure 6.10c) it can be seen that the weight fraction of the σ-phase is still increasing, reaching a value close to 2.9 (%wt). It can be noticed that the σ-phase precipitates are located, mainly, at δ to δ phase boundaries, within δ-phase, where favourable conditions are met to promote $\delta \rightarrow \sigma + \gamma_2$ eutectoid precipitation/decomposition, suggesting that the $\delta \rightarrow \sigma + \gamma_2$ eutectoid precipitation/decomposition tends to become the most influential σ-phase precipitation mechanism, an observation confirmed by the further observed increase in the ($\gamma + \gamma_2$) weight fraction, form 51.7(%wt) to 52.6(%wt) (see Table 6.10). In terms of average grain-size, it can observe that δ-phase, γ-phase and σ-phase show an increase to 74.5μm, 29.5μm and respectively, 8.2μm,

6.6.2. Solution treatment at 1050°C (ST2.2) state

Figure 6.11 shows the microstructural aspects obtained after applying a solution treatment at 1050°C, with a treatment duration of 20min (Figure 6.11a), 40min (Figure 6.11b) and 60min (Figure 6.11c). In the case of the solution treatment performed with a treatment duration of 20min (ST 2.2.1), it can be observed that the initially intensely deformed δ-phase and γ-phase grains are fully recrystallized, all grains showing uniform morphology and a very low defect density. The average grain-size of the γ-phase is close to 24.4μm while, the δ-phase is close to 63.5μm (see Table 6.11). No other precipitated secondary phases are observed. The overall average weight fraction of the observed γ-phase was situated close to 51.1 (%wt), while the average weight fraction of the δ-phase was close to 48.9 (%wt).

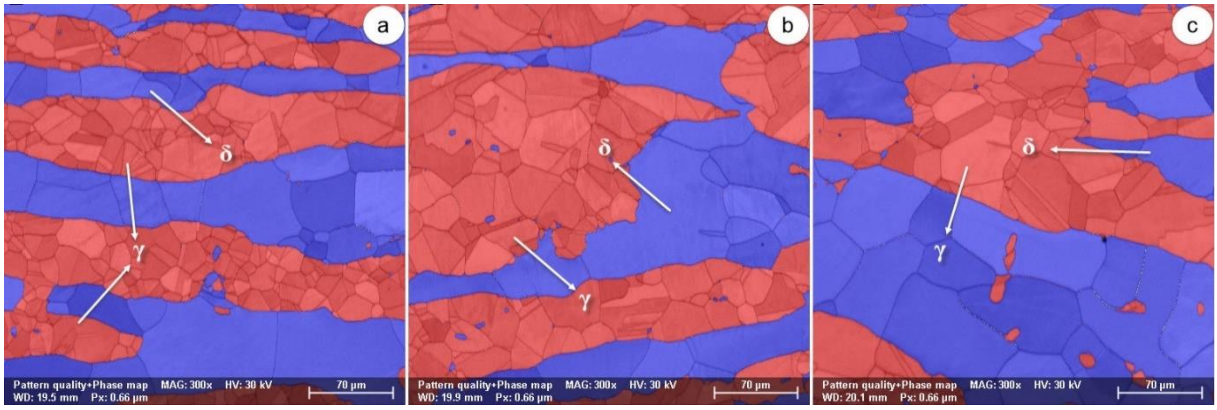

Fig. 6.11. *Characteristic SEM-EBSD microstructural images of solution treated samples at 1050°C (ST 2.2) state, with a treatment duration of 20min (ST 2.2.1) (a); 40min (ST 2.2.2) (b); 60min (ST 2.2.3) (c).*

Table 6.11

Average volume fraction [%wt] and average grain size [μm] for ST 2.2 state.

Structural state / Solution treatment at 1050°C (ST 2.2)	**Average volume fraction [%wt]**			**Average grain-size [μm]**		
	$\gamma + \gamma_2$	**δ**	**σ**	**$\gamma + \gamma_2$**	**δ**	**σ**
Solution treated: 1050°C/20mins/WQ (**ST 2.2.1**)	51.1	48.9	-	24.4	63.5	-
Solution treated: 1050°C/40mins/WQ (**ST 2.2.2**)	49.3	50.7	-	31.8	71.5	-
Solution treated: 1050°C/60mins/WQ (**ST 2.2.3**)	47.8	52.2	-	33.3	74.4	-

Increasing the treatment duration to 40min it can notice a small increase in the weight fraction of the δ-phase, from 48.9 (%wt) to 50.7 (%wt), suggesting that at this treatment duration the γ → δ phase transition is occurring. Also, it can notice that the average grain-size of the constituent γ-phase and δ-phase are increasing, from 24.4μm to 31.8μm and, respectively, from 63.5μm to 71.5μm, due to the grain-growth by diffusion mechanism (see Figure 6.11b and Table 6.11). Further increasing the treatment duration to 60min (Figure 6.11c) leads to a continuous increase in the weight fraction of the δ-phase, reaching 52.2 (%wt), confirming that at 1050°C and long enough durations the γ → δ phase transition is occurring and can be significant in terms of transformed weight fraction (see Table 6.11). Also, the noticed increase in the average grain-size of both constituent γ-phase and δ-phase, to 33.3μm and, respectively, 74.4μm (Table 6.11).

6.6.3. Solution treatment at 1100°C (ST2.3) state

Figure 6.12 shows the microstructural aspects obtained after applying a solution treatment at 1100°C, with a treatment duration of 20min (Figure 6.12a), 40min (Figure 6.12b) and 60min (Figure 6.12c).

In the case of the solution treatment performed with a treatment duration of 20min (ST 2.3.1) it can observe that the microstructure consists of fully recrystallized constituent γ-phase and δ-phase grains, all grains showing uniform morphology and a very low defect density. The average grain-size of the γ-phase is close to 20.4μm while, the δ-phase is close to 66.5μm (see Table 6.12). No other precipitated secondary phases are observed. The overall average weight fraction of the observed γ-phase was situated close to 47 (%wt), while the average weight fraction of the δ-phase was close to 53 (%wt) (see Table 6.12).

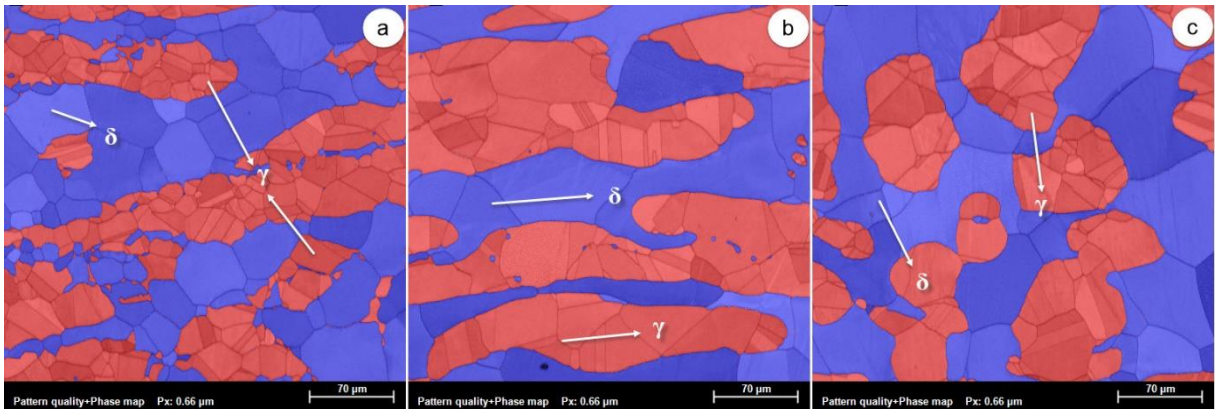

Fig. 6.12. *Characteristic SEM-EBSD microstructural images of solution treated samples at 1100°C (ST 2.3) state, with a treatment duration of 20min (ST 2.3.1) (a); 40min (ST 2.3.2) (b); 60min (ST 2.3.3) (c).*

Table 6.12

Average volume fraction [%wt] and average grain size [μm] for ST 2.3 state.

Structural state / Solution treatment at 1100°C (ST 2.3)	**Average volume fraction [%wt]**			**Average grain-size [μm]**		
	γ + γ2	**δ**	**σ**	**γ + γ2**	**δ**	**σ**
Solution treated: 1100°C/20mins/WQ (**ST 2.3.1**)	47.0	53.0	-	20.4	66.5	-
Solution treated: 1100°C/40mins/WQ (**ST 2.3.2**)	44.5	55.5	-	30.4	74.6	-
Solution treated: 1100°C/60mins/WQ (**ST 2.3.3**)	42.8	57.2	-	44.3	78.1	-

Increasing the treatment duration to 40min (ST 2.3.2) it can be noticed an increase in the weight fraction of the δ-phase, from 53(%wt) to 55(%wt), suggesting that at this treatment duration the γ → δ phase transition is occurring, showing a higher transformation rate

comparing with the solution treatment performed at 1050°C (ST 2.2) case. Also, it can be seen that the average grain-size of the constituent γ-phase and δ-phase are increasing, to 30.4μm and, respectively, to 74.6μm, indicting, also, that the grain-growth rate is higher compared with the solution treatment performed at 1050°C (ST 2.2) case (see Table 6.12).
Further increasing the treatment duration to 60min (ST 2.3.3) leads to a continuous increase in the weight fraction of the δ-phase, reaching 57.2 (%wt), confirming that at 1100°C and long enough durations the γ → δ phase transition is significant in terms of transformed weight fraction (see Table 6.12). Also, it can be noticed a significant increase in the average grain-size of both constituent γ-phase and δ-phase, to 44.3μm and, respectively, 78.1μm (see Figure 6.12c and Table 6.12).

6.7. Hot deformation at 1100ºC (HD3) state

The microstructural SEM-EBSD analysis of hot deformed, by rolling, at 1100°C (HD3) state is presented in Figure 6.13. It can observe that the applied intense (total applied deformation degree = 60%) hot deformation leads to the following observations, firstly, both initial δ and γ phases are showing signs of intense deformation secondly, no other precipitated secondary phases are observed, suggesting that the hot deformation temperature is situated above the threshold temperature to induce precipitation of the deleterious σ-phase (see Fig. 6.13a).
The analysis of variations in the average volume fraction of constituent phases shows that during hot deformation (at 1100°C) only in the case of δ-phase recorded small variations, confirming that the γ-phase contributes to δ-phase transition (see Table 6.13). The overall observed δ-phase weight fraction was close to 52.6 (%wt) and the austenite phase close to 47.4 (%wt), while the average grain-size was situated close to 113μm and 73.8 respectively (see Table 6.13).

Table 6.13

Average volume fraction [%wt] and average grain size [μm] for HD2 state.

Structural state	Average volume fraction [%wt]			Average grain-size [μm]		
	γ + γ2	δ	σ	γ + γ2	δ	σ
Hot deformed at 1100°C (**HR3**)	47.4	52.6	-	73.8	113	-

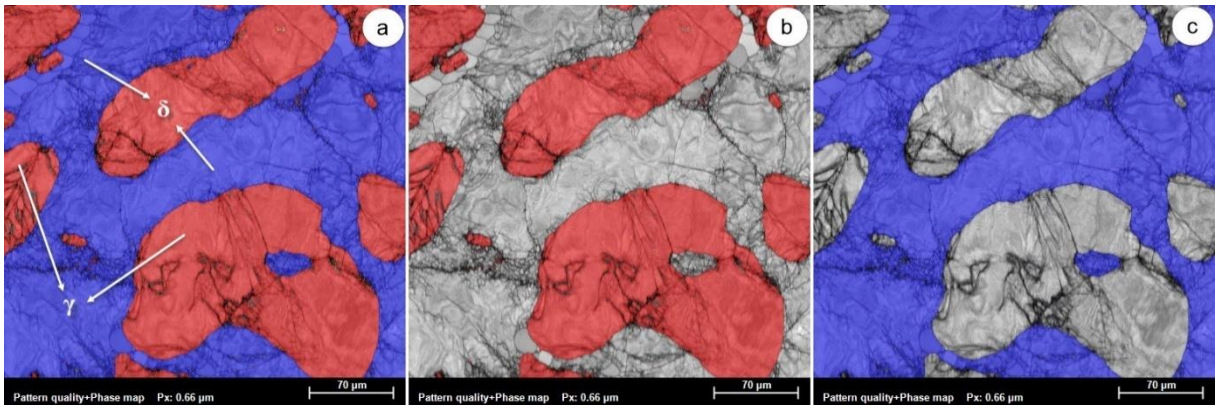

Fig. 6.13. *SEM-EBSD microstructure of hot-rolled at 1100ºC (HD3) state (a); austenite phase (b); ferrite phase (c).*

Morphological aspects of deformed δ and γ phases show the presence of intense deformed and fragmented grains also, the presence of strain-hardening phenomena within the microstructure. Comparing the δ-phase grains with the γ-phase grains, it can be observed that the γ-phase grains are showing signs of more intense fragmentation in comparison with the δ-phase grains, while δ-phase grains are showing signs of more intense strain-hardening in

comparison with the γ-phase grains. The computed average grain-size of both δ-phase and γ-phase shows that the fragmentation of the γ-phase grains is much more intense when compared to δ-phase grains, it can observe that the average grain-size of the γ-phase was situated close to 73.8 μm, while in theδ-phase case close to 113 μm (see Table 6.13).

6.8. Solution treatment at 1100°C (ST3) state

6.8.1. Solution treatment at 1000°C (ST3.1) state

Figure 6.14 shows the microstructural evolution as a result of applying a solution treatment at 1000°C, with a treatment duration of 20min (Figure 6.14a), 40min (Figure 6.14b) and 60min (Figure 6.14c). In the case of the solution treatment performed with a treatment duration of 20min (ST 3.1.1) it can observe that the initially intensely deformed δ-phase and γ-phase grains are fully recrystallized, all grains showing uniform morphology and a very low defect density. The average grain-size of the γ-phase is close to 26.1μm while, the δ-phase is close to 40.2μm. Besides the δ-phase and γ-phase it can be observed that the σ-phase is present in the microstructure, suggesting that the treatment duration is still low enough to assure precipitation of the σ-phase (Figure 6.14a).

Analysing the location of σ-phase precipitates it can be seen that, mainly, the precipitation occurred at δ to γ phase boundaries, within δ-phase, in sites where favourable conditions are met in order to promote a $\delta \rightarrow \sigma$ precipitation. Also, it can be noticed sites at δ to δ phase boundaries, within δ-phase, where favourable conditions are met in order to promote $\delta \rightarrow \sigma + \gamma_2$ eutectoid precipitation/decomposition. The overall observed σ-phase weight fraction was situated close to 2.9 (%wt), while the average grain-size was situated close to 4.7μm (see Table 6.14). The analysis of variations in the average volume fraction of constituent phases shows that during solution treatment (at 1000°C with a treatment duration of 20min) only in the case of δ-phase and σ-phase are recorded significant variations, confirming that the σ-phase is linked to the δ-phase and not linked to the γ-phase (see Table 6.14).

Increasing the treatment duration to 40min (Figure 6.14b) it can be noticed that the weight fraction of the σ-phase is increasing, being recorded close to 4.5(%wt). It can notice that the σ-phase precipitates are located, almost at δ to δ phase boundaries and less at δ to γ, suggesting that with treatment duration increment the precipitation mechanism is shifted towards $\delta \rightarrow \sigma + \gamma_2$ eutectoid precipitation/decomposition, an observation confirmed by the small increase observed in the ($\gamma + \gamma_2$) weight fraction, form 54.3(%wt) to 55.6(%wt) (see Table 6.14). In terms of average grain-size it can observe an increase δ phase, from 40.2μm to 58.6 μm and from 4.7μm to 6.8μm for σ-phase due to the grain-growth by diffusion mechanism. For the γ-phase average grain-size decreased, from 26.1μm to 22.7μm due to generating small grains of secondary austenite at δ to δ phase boundaries which affect the average grain size of the austenite phase (see Table 6.14).

Increasing the treatment duration to 60min (Figure 6.14c) it can be seen that the weight fraction of the σ-phase is still increasing, reaching a value close to 7.5 (%wt). It can be noticed that the σ-phase precipitates are located, mainly, at δ to δ phase boundaries, within δ-phase, where favourable conditions are meet in order to promote $\delta \rightarrow \sigma + \gamma_2$ eutectoid precipitation / decomposition, suggesting that the $\delta \rightarrow \sigma + \gamma_2$ eutectoid precipitation / decomposition tends to become the most influential σ-phase precipitation mechanism,

observation confirmed by further observed increase in the ($\gamma + \gamma_2$) weight fraction, form 55.6(%wt) to 57.9(%wt) (see Table 5.14).

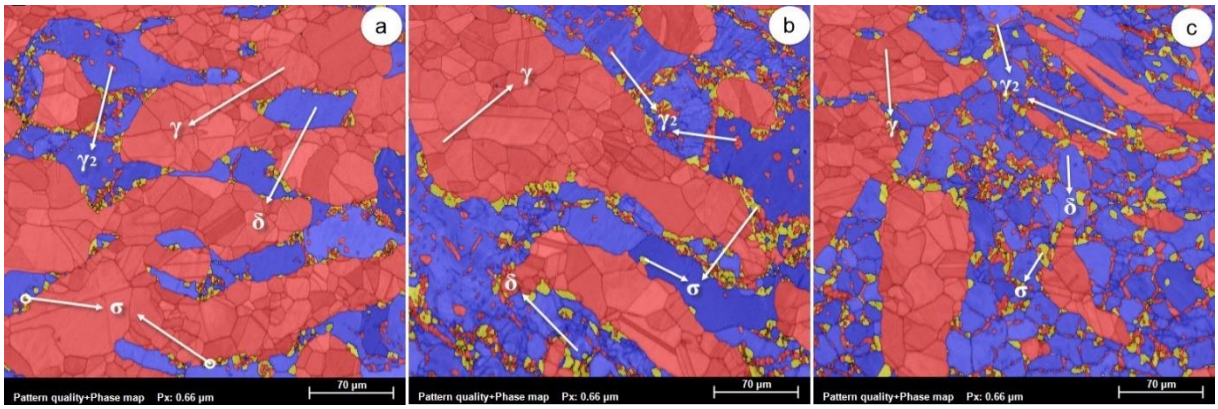

Fig. 6.14. *Characteristic SEM-EBSD microstructural images of solution treated samples at 1000°C (ST 3.1) state, with a treatment duration of 20min (ST 3.1.1) (a); 40min (ST 3.1.2) (b); 60min (ST 3.1.3) (c).*

Table 6.14

Average volume fraction [%wt] and average grain size [µm] for ST 3.1 state.

Structural state / Solution treatment at 1000ºC (ST 3.1)	**Average volume fraction [%wt]**			**Average grain-size [µm]**		
	$\gamma + \gamma_2$	**δ**	**σ**	**$\gamma + \gamma_2$**	**δ**	**σ**
Solution treated: 1000°C/20mins/WQ (**ST 3.1.1**)	54.3	42.8	2.9	26.1	40.2	4.7
Solution treated: 1000°C/40mins/WQ (**ST 3.1.2**)	55.6	39.9	4.5	22.7	58.6	6.8
Solution treated: 1000°C/60mins/WQ (**ST 3.1.3**)	57.9	34.6	7.5	19.1	55.7	7.1

In terms of average grain-size it can observe an increase σ-phase, from 6.8µm to 7.1µm due to the grain growth by diffusion mechanism. For γ-phase and δ-phase average grain-size decreased to 19.1 and respectively, 55.7µm due to generating small grains of secondary austenite at δ to δ phase boundaries which affect the average grain size of austenite phase (see Table 6.14).

6.8.2. Solution treatment at 1050°C (ST3.2) state

Figure 6.15 shows the microstructural aspects obtained after applying a solution treatment at 1050°C, with a treatment duration of 20min (Figure 5.15a), 40min (Figure 5.15b) and 60min (Figure 5.15c). In the case of the solution treatment performed with a treatment duration of 20min (ST 3.2.1), it can be observed that the initially intensely deformed δ-phase and γ-phase grains are fully recrystallized, all grains showing uniform morphology and a very low defect density (see Figure 6.15a). The average grain-size of the γ-phase is close to 36.7µm while, the δ-phase is close to 54.2µm (see Table 5.15). No other precipitated secondary phases are observed. The overall average weight fraction of the observed γ-phase was situated close to 54.4 (%wt), while the average weight fraction of the δ-phase was close to 45.6 (%wt) (see Figure 6.15a and Table 6.15).

Increasing the treatment duration to 40min (Figure 6.15b) one can see a small increase in the weight fraction of the δ-phase, from 45.6 (%wt) to 48.3 (%wt), suggesting that at this treatment duration the $\gamma \rightarrow \delta$ phase transition is occurring, but with a small transformation rate. Also, it can be noticed that the average grain-size of the constituent δ-phase is increasing, from 54.2µm to 71.5µm due to the grain growth by diffusion mechanism (see Figure 6.15b and Table 6.15). While the average grain-size of the constituent γ-phase decreased from 36.7µm to 33.8µm due to generating small secondary austenite grains γ_2

within ferrite phase at δ to δ phase boundaries which affect the average grain size of the austenite phase (see Table 6.15).

Further increasing the treatment duration to 60min (Figure 6.15c) leads to a continuous increase in the weight fraction of the δ-phase, reaching 50.8 (%wt), confirming that at 1050°C and long enough durations the γ → δ phase transition is occurring and can be significant in terms of transformed weight fraction (see Figure 15c and Table 6.15). Also, the noticed increase in the average grain-size of the constituent δ-phase, to 84.2μm confirms that the grains are growing due to the diffusion mechanism, while the γ-phase decreased to 30.9μm (see Figure 6.15c and Table 6.15) due to the increasing the generation of small secondary austenite grains γ_2 within ferrite phase (see Table 6.15).

Table 6.15

Average volume fraction [%wt] and average grain size [μm] for ST 3.2 state.

Structural state / Solution treatment at 1050ºC (ST 3.2)	**Average volume fraction [%wt]**			**Average grain-size [μm]**		
	γ + γ2	**δ**	**σ**	**γ + γ2**	**δ**	**σ**
Solution treated: 1050°C/20mins/WQ (**ST 3.2.1**)	54.4	45.6	-	36.7	54.2	-
Solution treated: 1050°C/40mins/WQ (**ST 3.2.2**)	51.7	48.3	-	33.8	71.5	-
Solution treated: 1050°C/60mins/WQ (**ST 3.2.3**)	49.2	50.8	-	30.9	84.2	-

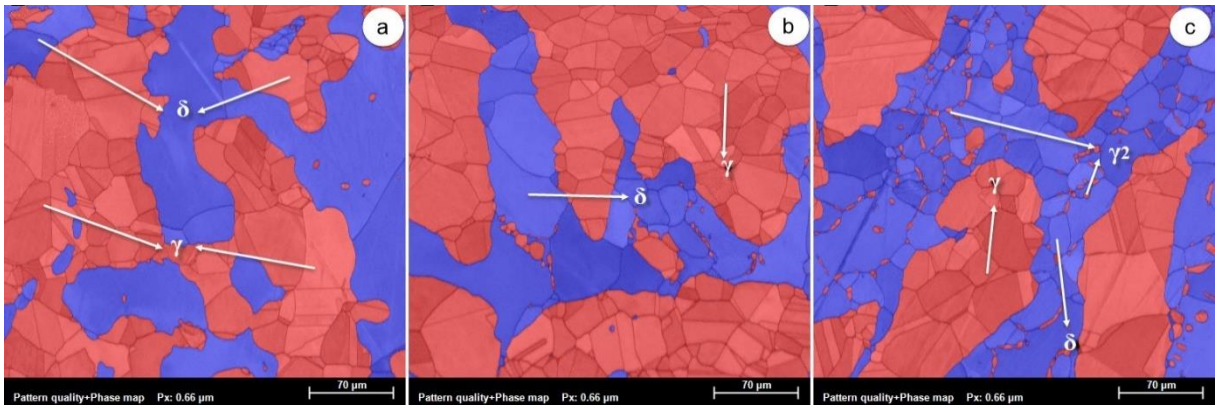

Fig. 6.15. *Characteristic SEM-EBSD microstructural images of solution treated samples at 1050°C (ST 3.2) state, with a treatment duration of 20min (ST 3.2.1) (a); 40min (ST 3.2.2) (b); 60min (ST 3.2.3) (c).*

6.8.3. Solution treatment at 1100°C (ST3.3) state

Figure 6.16 shows the microstructural aspects obtained after applying a solution treatment at 1100°C, with a treatment duration of 20min (Figure 6.16a), 40min (Figure 6.16b) and 60min (Figure 6.16c). In the case of the solution treatment performed with a treatment duration of 20min (ST 3.3.1) it can be observed that the microstructure consists of fully recrystallized constituent γ-phase and δ-phase grains, all grains showing uniform morphology and a very low defect density. The average grain-size of the γ-phase is close to 33.1μm while, the δ-phase is close to 72.5μm (see Table 6.16). No other precipitated secondary phases are observed. The overall average weight fraction of the observed γ-phase was situated close to 45.1 (%wt), while the average weight fraction of the δ-phase was close to 54.9 (%wt) (see Table 6.16).

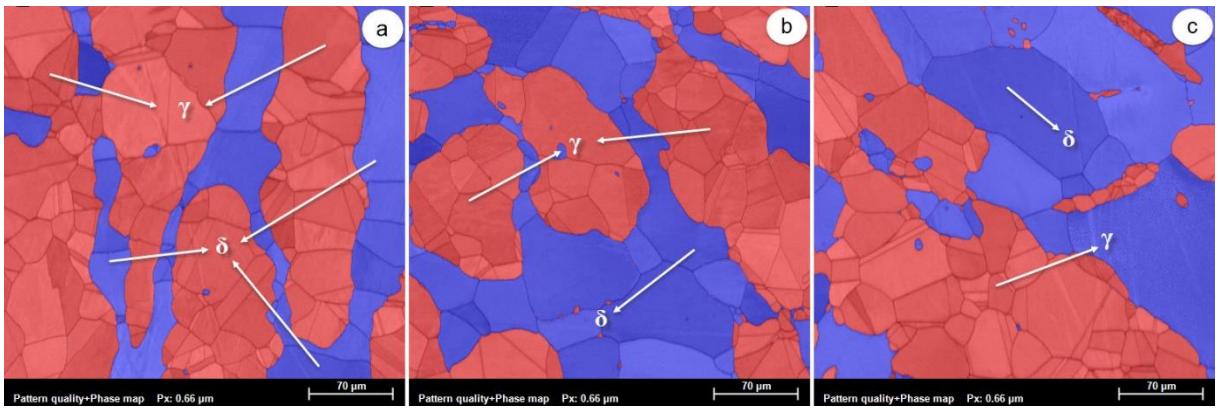

Fig. 6.16. *Characteristic SEM-EBSD microstructural images of solution treated samples at 1100°C (ST 3.3) state, with a treatment duration of 20min (ST 3.3.1) (a); 40min (ST 3.3.2) (b); 60min (ST 3.3.3) (c).*

Increasing the treatment duration to 40min (ST 3.3.2) (Figure 6.27b) one can see an increase in the weight fraction of the δ-phase, from 58.2 (%wt) to 41.8 (%wt), suggesting that at this treatment duration the γ → δ phase transition is occurring, but with a higher transformation rate comparing with the solution treatment performed at 1050°C (ST 3.2) case. Also, it can be noticed that the average grain-size of the constituent γ-phase and δ-phase are increasing, to 37.6µm and, respectively, to 87.5µm, indicting, also, that the grain-growth rate is higher compared with the solution treatment performed at 1050°C (ST 3.2) case (see Table 6.16).

Table 6.16

Average volume fraction [%wt] and average grain size [µm] for ST 3.3 state.

Structural state / Solution treatment at 1100ºC (ST 3.3)	**Average volume fraction [%wt]**			**Average grain-size [µm]**		
	γ + γ2	**δ**	**σ**	**γ + γ2**	**δ**	**σ**
Solution treated: 1100°C/20mins/WQ (**ST 3.3.1**)	45.1	54.9	-	33.1	72.5	-
Solution treated: 1100°C/40mins/WQ (**ST 3.3.2**)	41.8	58.2	-	37.6	87.5	-
Solution treated: 1100°C/60mins/WQ (**ST 3.3.3**)	38.9	61.1	-	40.1	107	-

Further increasing the treatment duration to 60min (ST 3.3.3) (Figure 6.16c) leads to a continuous increase in the weight fraction of the δ-phase, reaching 61.1 (%wt), confirming that at 1100°C and long enough durations the γ → δ phase transition is occurring and is significant in terms of transformed weight fraction. Also, can be seen a significant increase in the average grain-size of both constituents γ-phase and δ-phase, to 40.1µm and, respectively, 107µm (see Table 6.16).

6.9. Hot deformation at 1150ºC (HD4) state

The microstructural SEM-EBSD analysis of hot deformed, by rolling, at 1150°C (HD4) state is presented in Figure 6.17. It can be observed that the applied intense (total applied deformation degree = 60%) hot deformation leads to the following observations, firstly, both initial δ and γ phases are showing signs of intense deformation secondly, no other precipitated secondary phases are observed, suggesting that the hot deformation temperature is situated above the threshold temperature to induce precipitation of the deleterious σ-phase (see Fig. 6.17a).

The analysis of variations in the average volume fraction of constituent phases shows that during hot deformation (at 1150°C) only in the case of δ-phase recorded variations, confirming that the γ-phase contributes to δ-phase transition (see Table 6.17). The overall observed δ-phase weight fraction was close to 59.3 (%wt) and the austenite phase close to

40.7 (%wt), while the average grain-size was situated close to 119μm and 42.7 respectively (see Table 6.17).

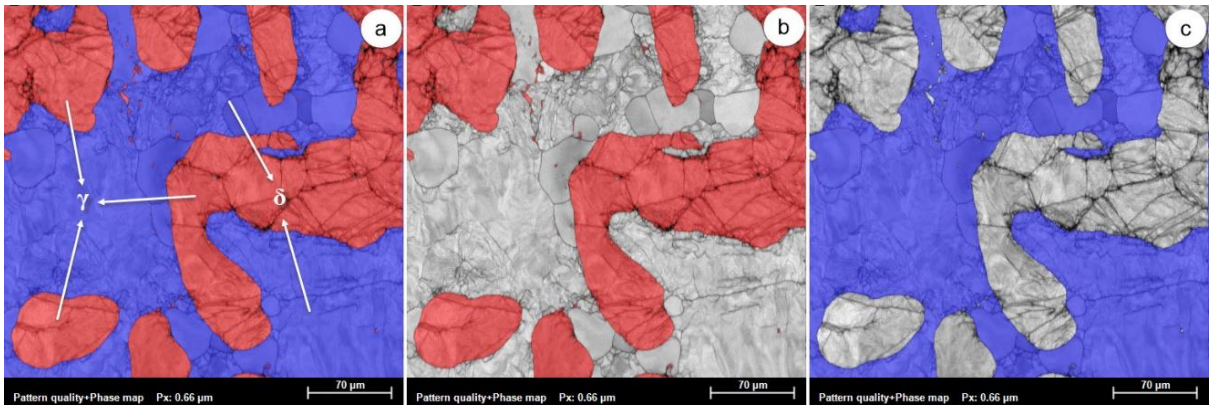

Fig. 6.17. *SEM-EBSD microstructure of hot-rolled at 1150ºC (HD4) state (a); austenite phase (b); ferrite phase (c).*

Table 6.17

Average volume fraction [%wt] and average grain size [μm] for HD4 state.

Structural state	Average volume fraction [%wt]			Average grain-size [μm]		
	γ + γ2	**δ**	**σ**	**γ + γ2**	**δ**	**σ**
Hot deformed at 1150°C (**HR4**)	40.7	59.3	-	42.7	119	-

Morphological aspects of deformed δ and γ phases show the presence of intense deformed and fragmented grains also, the presence of strain-hardening phenomena within the microstructure. Comparing the δ-phase grains with the γ-phase grains, it can be seen that the γ-phase grains are showing signs of more intense fragmentation in comparison with the δ-phase grains, while δ-phase grains are showing signs of more intense strain-hardening in comparison with the γ-phase grains. The computed average grain-size of both δ-phase and γ-phase shows that the fragmentation of the γ-phase grains is much more intense when compared to δ-phase grains, it can observe that the average grain-size of the γ-phase was situated close to 42.7 μm, while in theδ-phase case close to 119 μm (see Table 6.17).

6.10. Solution treatment at 1105°C (ST4) state

6.10.1. Solution treatment at 1000°C (ST4.1) state

Figure 6.18 shows the microstructural evolution as a result of applying a solution treatment at 1000°C, with a treatment duration of 20min (Figure 6.18a), 40min (Figure 6.18b) and 60min (Figure 6.18c). In the case of the solution treatment performed with a treatment duration of 20min (ST 4.1.1) it can be observed that the initially intensely deformed δ-phase and γ-phase grains are fully recrystallized, all grains showing uniform morphology and a very low defect density. The average grain-size of the γ-phase is close to 30.9μm while, the δ-phase is close to 45.5μm. Besides the δ-phase and γ-phase it can be seen that the σ-phase is present in the microstructure, suggesting that the treatment duration is still low enough to assure precipitation of the σ-phase (Figure 6.18a). Analysing the location of σ-phase precipitates it can be noticed that, mainly, the precipitation occurred at δ to γ phase boundaries, within δ-phase, in sites where favourable conditions are met in order to promote a δ → σ precipitation. Also, it can be seen sites at δ to δ phase boundaries, within δ-phase, where favourable conditions are met in order to promote δ → σ + γ_2 eutectoid precipitation/decomposition. The

overall observed σ-phase weight fraction was situated close to 1.5 (%wt), while the average grain-size was situated close to 4.4μm (see Table 6.18). The analysis of variations in the average volume fraction of constituent phases shows that during solution treatment (at 1000°C with a treatment duration of 20min) only in the case of δ-phase and σ-phase are recorded significant variations, confirming that the σ-phase is linked to the δ-phase and not linked to the γ-phase (see Table 6.18).

Increasing the treatment duration to 40min (Figure 6.18b) it can be seen that the weight fraction of the σ-phase is increasing, being recorded close to 2.4 (%wt). It can be noticed that the σ-phase precipitates are located, almost at δ to δ phase boundaries and less at δ to γ, suggesting that with treatment duration increment the precipitation mechanism is shifted towards δ → σ + γ_2 eutectoid precipitation/decomposition, an observation confirmed by the small increase observed in the (γ + γ_2) weight fraction, form 55.5(%wt) to 56.3(%wt) (see Table 6.18). In terms of average grain-size it can observe a decrease δ phase, from 45.5μm to 34.4 μm and from 30.9μm to 24.6μm for (γ + γ_2)-phase due to generating small grains of secondary austenite at δ to δ phase boundaries which affect the average grain size of austenite phase (see Figure 6.18b, Table 6.18). For σ-phase average grain-size increase, from 4.4μm to 5.2 μm due to grain-growth by diffusion mechanism (see Table 5.18).

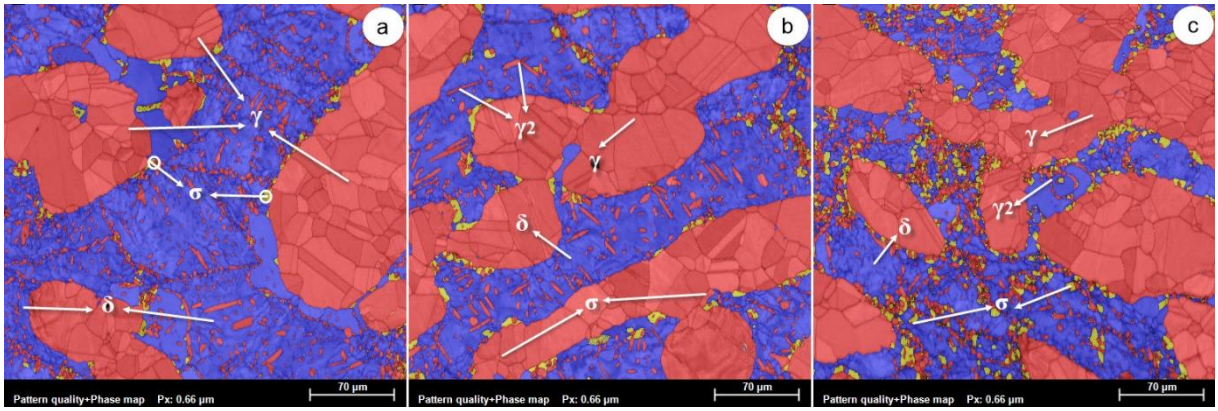

Fig. 6.18. *Characteristic SEM-EBSD microstructural images of solution treated samples at 1000°C (ST 4.1) state, with a treatment duration of 20min (ST 4.1.1) (a); 40min (ST 4.1.2) (b); 60min (ST 4.1.3) (c).*

Table 6.18

Average volume fraction [%wt] and average grain size [μm] for ST 4.1 state.

Structural state / Solution treatment at 1000ºC (ST 4.1)	**Average volume fraction [%wt]**			**Average grain-size [μm]**		
	γ + γ_2	**δ**	**σ**	**γ + γ_2**	**δ**	**σ**
Solution treated: 1000°C/20mins/WQ (**ST 4.1.1**)	55.5	43.0	1.5	30.9	45.5	4.4
Solution treated: 1000°C/40mins/WQ (**ST 4.1.2**)	56.3	41.3	2.4	24.6	34.4	5.2
Solution treated: 1000°C/60mins/WQ (**ST 4.1.3**)	57.1	37.4	5.5	19.9	28.7	6.2

Increasing the treatment duration to 60min (Figure 6.18c) it can notice that the weight fraction of the σ-phase is still increasing, reaching a value close to 5.5 (%wt). It can be noticed that the σ-phase precipitates are located, mainly, at δ to δ phase boundaries, within δ-phase, where favourable conditions are met to promote δ → σ + γ_2 eutectoid precipitation/ decomposition, suggesting that the δ → σ + γ_2 eutectoid precipitation/ decomposition tends to become the most influential σ-phase precipitation mechanism, an observation confirmed by the further observed increase in the (γ + γ_2) weight fraction, form 56.3(%wt) to 57.1(%wt)

(see Table 6.18). In terms of average grain-size it can observe an increase σ-phase, from 5.2μm to 6.2μm due to the grain-growth by diffusion mechanism.

For γ-phase and δ-phase average grain-size decrease to 19.9μm and respectively, 28.7μm due to generating small grains of secondary austenite at δ to δ phase boundaries which affect the average grain size of the austenite phase (see Table 6.18).

6.10.2. Solution treatment at 1050°C (ST4.2) state

Figure 6.19 shows the microstructural aspects obtained after applying a solution treatment at 1050°C, with a treatment duration of 20min (Figure 6.19a), 40min (Figure 6.19b) and 60min (Figure 6.19c). In the case of the solution treatment performed with a treatment duration of 20min (ST 4.2.1) it can be noticed that the initially intensely deformed δ-phase and γ-phase grains are fully recrystallized, all grains showing uniform morphology and a very low defect density (see Figure 6.19a). The average grain-size of the γ-phase is close to 33.2μm while, the δ-phase is close to 63.9μm (see Table 6.19). No other precipitated secondary phases are observed. The overall average weight fraction of the observed γ-phase was situated close to 47.9 (%wt), while the average weight fraction of the δ-phase was close to 52.1 (%wt) (see Table 6.19).

Increasing the treatment duration to 40min (Figure 6.19b) it can notice a small increase in the weight fraction of the δ-phase, from 52.1 (%wt) to 53.9 (%wt), suggesting that at this treatment duration the γ → δ phase transition is occurring, but with a small transformation rate. Also, it can be seen that the average grain-size of the constituent δ-phase is increasing, from 63.9μm to 87.9μm due to the grain-growth by diffusion mechanism (see Figure 6.19b and Table 6.19). While the average grain-size of the constituent γ-phase decreased from 33.2μm to 31.5μm due to generating small secondary austenite grains γ_2 within ferrite phase at δ to δ phase boundaries which affect the average grain size of the austenite phase (see Table 6.19).

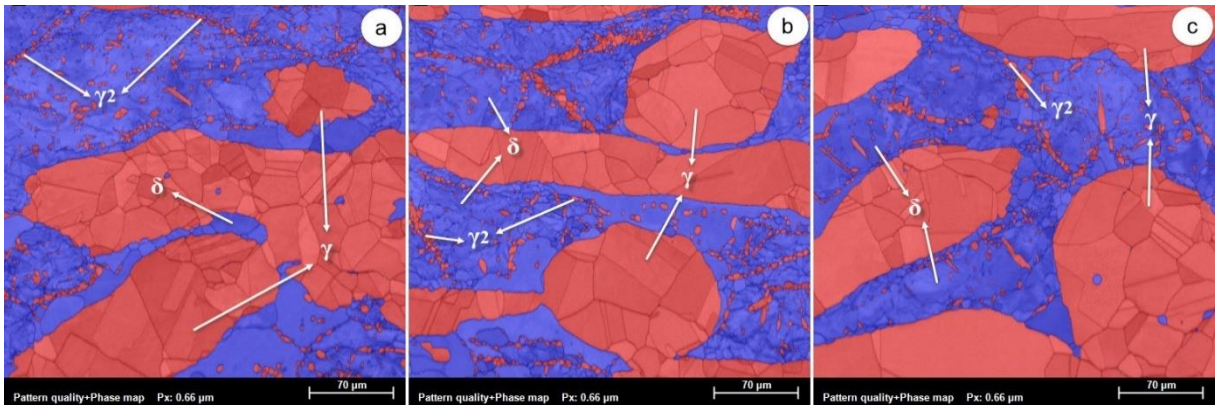

Fig. 6.19. *Characteristic SEM-EBSD microstructural images of solution treated samples at 1050°C (ST 4.2) state, with a treatment duration of 20min (ST 4.2.1) (a); 40min (ST 4.2.2) (b); 60min (ST 4.2.3) (c).*

Further increasing the treatment duration to 60min (Figure 6.19c) leads to a continuous increase in the weight fraction of the δ-phase, reaching 55.8 (%wt), confirming that at 1050°C and long enough durations the γ → δ phase transition is occurring and can be significant in terms of transformed weight fraction (see Table 6.19). Also, the noticed increase in the average grain-size of constituent δ-phase, to 103μm confirming that the grains are growing due to the diffusion mechanism, while the γ-phase decreased to 30.8μm due to

the increasing the weight fraction of small secondary austenite grains γ_2 within ferrite phase (see Figure 6.19b).

Table 6.19

Average volume fraction [%wt] and average grain size [μm] for ST 4.2 state.

Structural state / Solution treatment at 1050ºC (ST 4.2)	Average volume fraction [%wt]			Average grain-size [μm]		
	$\gamma + \gamma_2$	**δ**	**σ**	**$\gamma + \gamma_2$**	**δ**	**σ**
Solution treated: 1050°C/20mins/WQ (**ST 4.2.1**)	47.9	52.1	-	33.2	63.9	-
Solution treated: 1050°C/40mins/WQ (**ST 4.2.2**)	46.1	53.9	-	31.5	87.9	-
Solution treated: 1050°C/60mins/WQ (**ST 4.2.3**)	44.2	55.8	-	30.8	103	-

6.10.3. Solution treatment at 1100°C (ST4.3) state

Figure 6.20 shows the microstructural aspects obtained after applying a solution treatment at 1100°C, with a treatment duration of 20min (Figure 6.20a), 40min (Figure 6.20b) and 60min (Figure 6.20c). In the case of the solution treatment performed with a treatment duration of 20min (ST 4.3.1) it can be observed that the microstructure consists of fully recrystallized constituent γ-phase and δ-phase grains, all showing uniform morphology and a very low defect density. The average grain-size of the γ-phase is close to 33.5μm while, the δ-phase is close to 80.8μm. No other precipitated secondary phases are observed. The overall average weight fraction of the observed γ-phase was situated close to 43.1 (%wt), while the average weight fraction of the δ-phase was close to 56.9 (%wt) (see Table 6.20).

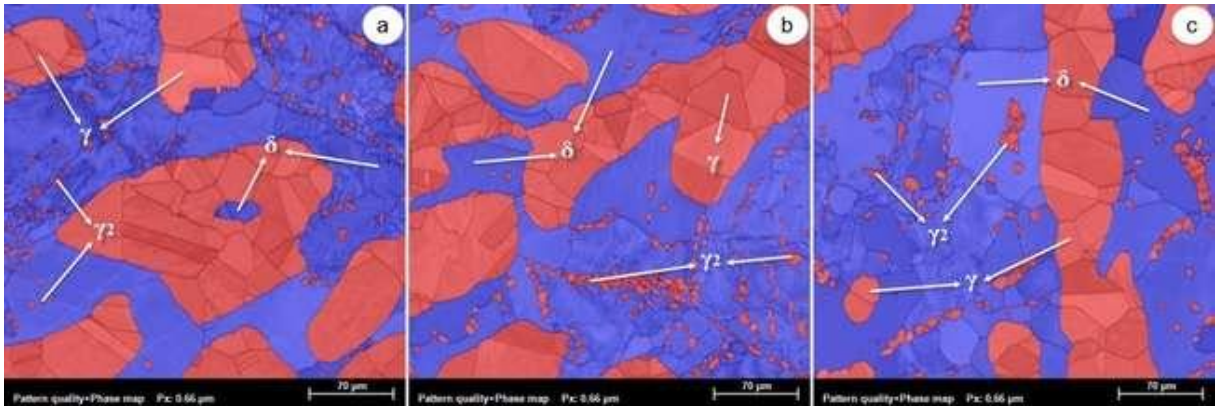

Fig. 6.20. *Characteristic SEM-EBSD microstructural images of solution treated samples at 1100°C (ST 4.3) state, with a treatment duration of 20min (ST 4.3.1) (a); 40min (ST 4.3.2) (b); 60min (ST 4.3.3) (c).*

Increasing the treatment duration to 40min (ST 4.3.2) (Figure 6.20b) one can see an increase in the weight fraction of the δ-phase, from 56.9 (%wt) to 60.4 (%wt), suggesting that at this treatment duration the γ → δ phase transition is occurring, showing a higher transformation rate comparing with the solution treatment performed at 1050°C (ST 4.2) case. Also, it can be noticed that the average grain-size of the constituent γ-phase and δ-phase are increasing, to 38.8μm and, respectively, to 106μm, indicting, also, that the grain-growth rate is higher compared with the solution treatment performed at 1050°C (ST 4.2) case (see Table 6.19).

Further increasing the treatment duration to 60min (ST 4.3.3) (Figure 6.20c) leads to a continuous increase in the weight fraction of the δ-phase, reaching 61.1 (%wt), confirming that at 1100°C the γ → δ phase transition is occurring and is significant in terms of transformed weight fraction. Also, it can notice an increase in the average grain-size of both constituents γ-phase and δ-phase, to 40.6μm and, respectively 112μm (see Table 6.20).

Table 6.20

Average volume fraction [%wt] and average grain size [μm] for ST 4.3 state.

Structural state / Solution treatment at 1100ºC (ST 4.3)	Average volume fraction [%wt]			Average grain-size [μm]		
	$\gamma + \gamma_2$	δ	σ	$\gamma + \gamma_2$	δ	σ
Solution treated: 1100°C/20mins/WQ (**ST 4.3.1**)	43.1	56.9	-	33.5	80.8	-
Solution treated: 1100°C/40mins/WQ (**ST 4.3.2**)	39.6	60.4	-	38.8	106	-
Solution treated: 1100°C/60mins/WQ (**ST 4.3.3**)	33.3	66.7	-	40.6	112	-

6.11. Conclusions

The following conclusions arise from the advanced analysis of the microstructural evolution during thermomechanical processing of F55 SDSS alloy:

- The austenite (γ) phase is accommodating the applied deformation better compared to the ferrite (δ) phase, by slip/twinning, for the same applied stress/strain level, due to its easier to activate slip/twinning on its higher atomic density planes of the FCC crystalline system (γ-phase) compared with the BCC crystalline system (δ-phase);
- Increasing the deformation temperature, from 1000°C (HD 1) to 1150°C (HD 4), leads to an increase in the deformability of the ferrite (δ) phase;
- Increasing the deformation temperature, from 1000°C (HD 1) to 1150°C (HD 4), leads to an increase in the defects density in both the austenite (γ) and the ferrite (δ) phases;
- An increase in hot-deformation temperature, from 1000°C (HD 1) to 1150°C (HD 4), leads to an increase in the average weight fraction of the ferrite (δ) phase, from 45.8wt% (HD 1) to 59.3wt% (HD 4) and, to decrease in the average weight fraction of the austenite (γ) phase, from 50.7wt% (HD 1) to 40.7wt% (HD 4), due to the increase kinetics of the $\gamma \rightarrow \delta$ phase transition;
- The sigma (σ) phase precipitates were detected in the characteristic microstructures of hot-deformed samples at 1000°C (HD 1) and 1050°C (HD 2) states;
- Applying a solution treatment, from 1000°C to 1100°C, after hot deformation, leads to regeneration of both parent austenite (γ) and ferrite (δ) phases, all showing a low density of defects, no in-grain rotations/deflections and, low residual strain-stress fields;
- Sigma (σ) phase precipitates resulting during solution treatment were identified only at a treatment temperature of 1000°C (ST1.1, ST2.1, ST3.1 and ST4.1); two precipitation mechanisms were observed, firstly, σ-phase precipitation occurred at δ to γ phase boundaries, within δ-phase, by the $\delta \rightarrow \sigma$ transformation and, secondly, σ-phase precipitation occurred at δ to δ phase boundaries, within δ-phase, by the $\delta \rightarrow \sigma + \gamma_2$ eutectoid precipitation/decomposition transformation;
- An increase in the solution treatment duration, from 20min to 60min, in the case of solution treatments performed at 1000°C (ST 1.1, ST 2.1, ST 3.1 and ST 4.1), leads to an increase in both grain-size and weight fraction of the precipitated sigma (σ) phase; the highest average grain-size (7.1μm) and weight fraction (7.5wt%) being recorded for the samples hot-deformed at 1100°C (HD 3) and solution treated at 1000°C for 60 min (ST 3.1.3);
- An increase in the solution treatment temperature, from 1000°C to 1100°C, leads to an increase in average grain-size of both the austenite (γ) and the ferrite (δ) phases; the

highest values being recorded in the case of samples hot deformed at 1150°C (HD 4) and solution treated at 1100°C for 60min (ST 4.3.3), when the average grain-size of the austenite was close to 40.6μm while the ferrite close to 112μm;

- An increase in the solution treatment temperature, from 1000°C to 1100°C, leads to an increase in the average weight fraction of the ferrite (δ) phase and, a decrease in the average weight fraction of the austenite (γ) phase; the highest average weight fraction of the ferrite phase being recorded in the case of samples hot deformed at 1150°C (HD 4) and solution treated at 1100°C for 60min (ST 4.3.3) - close to 66.7wt%, while the average weight fraction of the austenite phase - close to 33.3wt%;
- Annealing twins are formed within the austenite (γ) phase during solution treatment

Chapter 7: Mechanical properties evolution during thermomechanical processing of F55 SDSS alloy

7.1. Introduction

Chapter 7 is focused on the advanced analysis of the mechanical properties evolution as a result of the applied thermomechanical processing routes, which assumed, firstly, a hot-deformation (at different temperatures: 1000°C; 1050°C; 1100°C; 1150°C) and, secondly, a solution treatment (at different temperatures: 1000°C; 1050°C; 1100°C; and different treatment durations: 20min; 40min; 60min) (see Fig. 7.1).

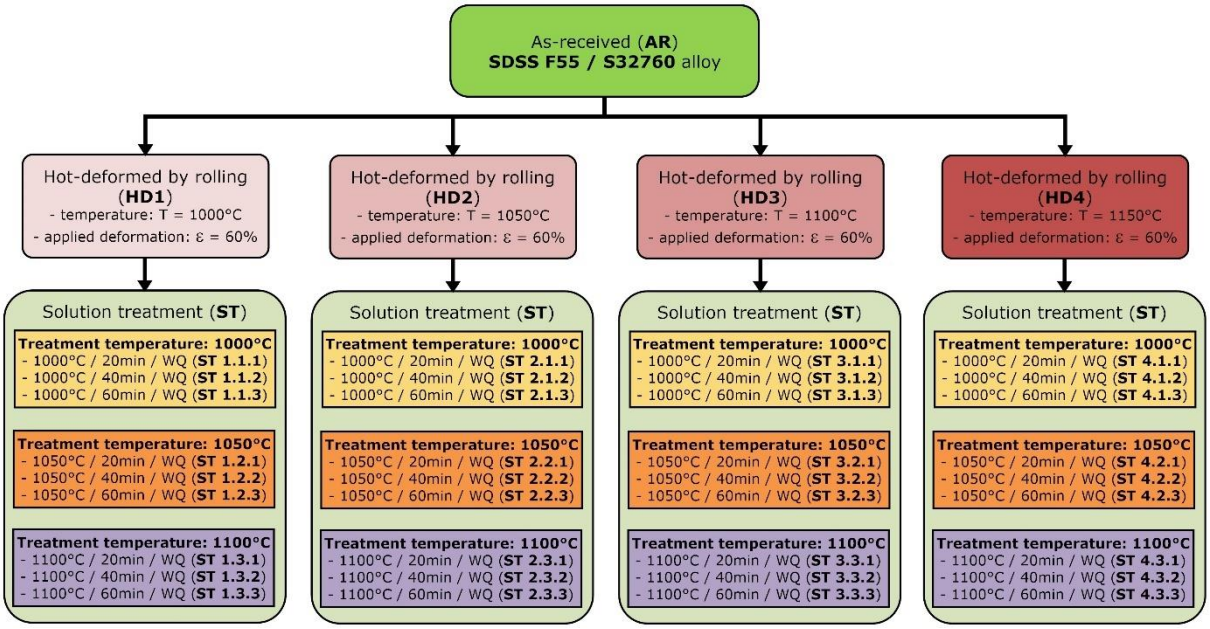

Fig. 7.1 *Thermomechanical processing route applied to the F55 (UNS S32760) SDSS alloy.*

Since every mechanical system is subjected to loads during operation, it is of utmost importance to understand how the materials, that make up these mechanical systems, behave. Also, the different thermomechanical processing parameters lead to obtaining different microstructural features (i.e., phase nature and phase structure, volume fraction, grain-size, internal micro-strain fields, etc) and, as a consequence, different mechanical behaviour.

The mechanical properties characterization can be performed using the following investigation techniques: tensile testing, compressive testing, impact testing, microhardness testing, etc. Based on these investigation techniques, it can be obtained important data

concerning the material's strength (0.2 yield strength - $\sigma_{0.2}$, ultimate tensile strength - σ_{UTS}, microhardness -HV0.1) and ductility properties(elongation to fracture - ε_f, etc).

The fracture surface analysis can be employed to investigate the predominant fracture mechanism which leads to the specimen failure during mechanical testing.

7.2. As-received (AR) state

Based on the strain-stress diagram obtained during tensile testing, it can be computed the following mechanical parameters: 0.2 yield strength - $\sigma_{0.2}$, ultimate tensile strength - σ_{UTS} and elongation to fracture - ε_f.

By using the microhardness testing technique, it can be obtained data concerning the alloy's overall microhardness (if the microhardness print is large enough to fit multiple phases at the same time) or the microhardness of individual constituent phases (if the microhardness print is small enough to fit the respective phase). In order to determine the microhardness of the constituent ferrite (δ) and austenite (γ) phases, the microhardness testing was performed using a testing force of 100g (see Fig. 7.2a and 7.2b), while the overall/global microhardness of the sigma (σ) phase + secondary austenite (γ_2) phases was determined using a testing force of 25g (see Fig. 7.2c) due to the small grain-size of the sigma (σ) phase.

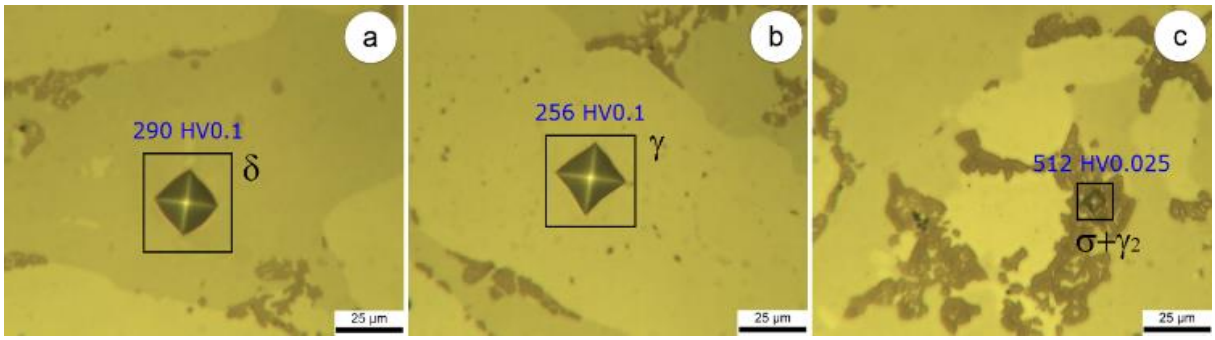

Figure 7.2 *Optical images of microhardness print of ferrite (δ) phase (a), austenite (γ) phase (b) and sigma and secondary austenite ($\sigma+\gamma_2$) phases (c).*

Table 7.1 presents the obtained mechanical properties for the as-received (AR) F55 SDSS alloy.

Table 7.1

Mechanical properties of as-received (AR) F55 SDSS alloy.

Structural state	Mechanical properties					
	Microhardness			σ_{UTS} [MPa]	$\sigma_{0.2}$ [MPa]	ε_f [%]
	δ [HV0.1]	γ [HV0.1]	$\sigma+\gamma_2$ [HV0.025]			
As-received **(AR)** sample	300±7	264±8	-	733±9	478±11	55±3

It can be observed that the AR condition shows high strength properties, ultimate tensile strength σ_{UTS} = 733MPa and yield strength $\sigma_{0.2}$ = 478MPa, coupled with high ductility, elongation to fracture ε_f = 55%, proving that the F55 alloy exhibits a good combination of properties due to the approximately equal weight fractions of constituent δ and γ phases, considering that the δ is "responsible" for the strength properties while the γ phase for the ductility properties [107].

As shown in Table 7.1, the microhardness of the constituent δ phase (300HV0.1) is higher than that of the constituent γ phase (264HV0.1). This can be explained, firstly, based on the

crystallography of constituent phases, being known that the BCC crystalline system inherently shows a higher microhardness compared with the FCC system, due to its higher necessary stress to accommodate elastic/plastic deformation and, secondly, based on the chemistry of the constituent phases, the δ phase being "richer" in harder chromium (Cr) content (~ 28.5wt%) comparing with the γ phase (~25.7wt%) (see Table 6.2 and 6.3).

7.3. Hot deformation at 1000ºC (HD1) state

Table 7.2 presents the obtained mechanical properties of F55 SDSS alloy due to the hot deformation at 1000°C (HD1). Compared with the AR state, it can be observed that the strength properties are showing a small increase, i.e., ultimate tensile strength σ_{UTS} = 768MPa and yield strength $\sigma_{0.2}$ = 524MPa, while the ductility properties, i.e., elongation to fracture ε_f = 34%, are showing a high decrease. This behaviour can be explained based on the microstructural changes that occurred during hot deformation. During deformation, the fragmentation of the grains occurs, leading to smaller size grains, grains rotations and a higher / increased defect density, in order to accommodate the applied strain/stress field. As shown in chapter 6.3, it can be noticed that due to the intensely deformed δ-phase and γ-phase grains, the strain-hardening phenomena occur, leading to an increase in strength and decrease in ductility.

Also, one must consider the influence of the precipitated deleterious σ-phase, being known that the small-size σ-phase precipitates can act as strengthening particles. It is known that the σ-phase precipitates can lead to a small increase in strength, a small decrease in ductility and a high decrease in toughness properties, even for small wight fractions [108-109].

As shown in Table 7.2, it can be observed that the microhardness of both constituents δ and γ phases are increasing, to 312HV0.1 and respectively 322HV0.1, due to the strain hardening that occurred during deformation. The higher microhardness recorded in the case of the γ-phase proves that the γ-phase grains are more strain-hardened, showing a higher defects density compared with the δ phase.

Table 7.2

Mechanical properties of HD1 state.

Structural state	Mechanical properties					
	Microhardness			σ_{UTS} [MPa]	$\sigma_{0.2}$ [MPa]	ε_f [%]
	δ [HV0.1]	γ [HV0.1]	σ+γ2 [HV0.025]			
Hot-rolled (**HD1**) at 1000°C	312±9	322±12	474±15	768±12	524±9	34±3

This behaviour resides in the crystallography of the FCC γ-phase compared with the BCC δ-phase, which accommodates better the applied strain/stress field by slip/twinning on its higher atomic density planes for the same applied stress/strain level [110-111]. Also, it must consider the presence of precipitated σ phase, which is forms, eighter by precipitation (δ → σ) or by eutectoid decomposition (δ → σ + γ_2). As shown in Table 7.2, it can be observed that the global microhardness of the (σ + γ_2) is reaching 474HV0.025. It has been shown that the chemistry of the σ-phase possesses an increased weight fraction of Cr, Mo, and other alloying elements and, therefore, a higher microhardness compared with the one of the parent δ-phase, reaching values from 400HV to 800HV [112-113].

7.4. Solution treatment (ST1) state

7.4.1. Solution treatment at 1000°C (ST1.1) state

Table 7.3 presents the obtained mechanical properties after applying a solution treatment at 1000°C (ST 1.1), with a variable treatment duration of 20min (ST 1.1.1), 40min (ST 1.1.2) and 60min (ST 1.1.3), on the hot deformation at 1000°C (HD1) samples. Compared with the HD1 state, it can observe that the strength properties are showing a small decrease in the case of both ultimate tensile strength (σ_{UTS}) and yield strength ($\sigma_{0.2}$) and, also, in the case of elongation to fracture (ε_f). The ultimate tensile strength (σ_{UTS}) is continuously decreasing, from 772MPa (ST 1.1.1) to 769MPa (ST 1.1.2) and, finally, to 732MPa (ST 1.1.3), while the yield strength ($\sigma_{0.2}$) from 460MPa to 449MPa and, finally, to 445MPa. The elongation to fracture (ε_f) is, also, continuously decreasing from 53% (ST 1.1.1) to 50% (ST 1.1.2) and, finally, to 43% (ST 1.1.3) (see Table 7.3).

The microhardness evolution of all δ, γ and ($\sigma+\gamma_2$) constituent phases shows that the microhardness exhibits no significant changes, minimal variations are occurring while increasing solution treatment duration, all values being within the dispersion variation (see Table 7.3). Overall, can be observed that the δ phase shows a microhardness varying within 281HV0.1 to 294HV0.1 range, γ phase showing a smaller microhardness compared with the δ phase, varying within 254HV0.1 to 277HV0.1 range and, ($\sigma+\gamma_2$) microhardness varying within 512HV0.025 to 522HV0.025 range.

Table 6.3

Mechanical properties of ST 1.1 state.

Structural state / Solution treatment at 1000ºC (ST 1.1)	**Mechanical properties**					
	Microhardness			**σ_{UTS}** [MPa]	**$\sigma_{0.2}$** [MPa]	**ε_f** [%]
	δ [HV0.1]	**γ** [HV0.1]	**$\sigma+\gamma_2$** [HV0.025]			
Solution treated: 1000°C/20mins/WQ (**ST 1.1.1**)	289±18	256±14	512±21	772±14	460±11	53±3
Solution treated: 1000°C/40mins/WQ (**ST 1.1.2**)	294±23	254±18	522±29	769±12	449±10	50±2
Solution treated: 1000°C/60mins/WQ (**ST 1.1.3**)	281±27	277±24	518±15	732±9	445±12	43±4

This observed mechanical behaviour must be explained considering the occurred microstructural changes during applied solution treatment. The explanation must consider the following competing mechanisms, firstly, the law of phase mixture of constituent phases and, secondly, the Hall-Pech grain-size influence.

According to the law of phase mixture states, the exhibited properties are proportionally influenced by the weight fraction of a particular phase [114]. Considering the specific case of the SDSS alloys, it was shown that the γ-phase is responsible for the plasticity/ductility while the δ-phase is responsible for the strength properties [108]. Also, it was shown that the precipitation of the σ-phase influenced all exhibited mechanical properties by inducing embrittlement [115]. As shown in chapter 6.4.1, it can notice that due to the applied solution treatment, besides the δ and γ phases, the deleterious σ phase is induced too. Also, it can be noticed that the wight fraction of the σ-phase is increasing with treatment duration increasing, from 2.7wt% (ST 1.1.1) to 3.5wt% (ST 1.1.2) and, finally, to 5.5wt% (ST 1.1.3), diminishing all exhibited mechanical properties (strength/ductility) (see Table 7.3).

The Hall-Pech influence shows that the mechanical behaviour of a certain phase is governed by a grain-size relation [116-117]:

$$\sigma_y = \sigma_0 + k \times \frac{1}{\sqrt{D}}$$

where: σ_y - yield stress; σ_0 - yield stress of a coarse-grained polycrystal; k - material constant; D - average grain-size of considered phase.

Also, has been noticed that a smaller average grain-size of a phase will lead to an increase in the phase's ductility, due to the increased number of grains which will participate in the accommodation of the applied strain-stress field (total boundary area per unit volume) [118].

Based on the Hall-Pech relation, it can be assumed that both strength and ductility properties of a phase are increasing with the decrease of the average grain-size of the respective phase.

As shown in chapter 6.4.1 (see Table 6.5), it can notice that small variations in the average grain-size of constituent phases are occurring during solution treatment (ST 1.1). Analysing the case of the δ-phase can be observed a small increase from 51.8μm (ST 1.1.1) to 54.9μm (ST 1.1.2) and, finally, to 57.7μm (ST 1.1.3), from 15.1μm (ST 1.1.1) to 19.6μm (ST 1.1.2) and, finally, to 16.6μm (ST 1.1.3) in the case of γ-phase and, from 4.9μm (ST 1.1.1) to 5.5μm (ST 1.1.2) and, finally, to 6.0μm (ST 1.1.3) in the case of σ-phase. According to the Hall-Pech relation, those small increases in the average grain-sizes of the constituent phases will lead to an, overall, decrease in alloy's strength and ductility properties (see Table 7.3).

7.4.2. Solution treatment at 1050°C (ST1.2) state

Table 7.4 presents the obtained mechanical properties after applying a solution treatment at 1050°C (ST 1.2), with a variable treatment duration of 20min (ST 1.2.1), 40min (ST 1.2.2) and 60min (ST 1.2.3), on the hot deformation at 1000°C (HD1) samples.

Analysing the effects induced by applying a solution treatment at 1050°C (ST 1.2) with a variable treatment duration of 20min (ST 1.2.1) it can be noticed that an increase in alloy overall mechanical properties is obtained. The ultimate tensile strength (σ_{UTS}) was increased, from 768MPa (HD1 state) to 793MPa (ST 1.2.1 state) and, the elongation to fracture (ε_f) from 34% (HD1 state) to 61% (ST 1.2.1 state), indicating that the newly recrystallized microstructure has removed the unwanted/deleterious effects induced by the previous intense plastic deformation.

Analysing the influence of increasing the solution treatment duration from 20min (ST 1.2.1) to 40min (ST 1.2.2) and, finally, to 60min (ST 1.2.3), it can be noticed that both strength and ductility properties are decreasing. Also, it can be observed that the ultimate tensile strength (σ_{UTS}) is continuously decreasing from 793MPa (ST 1.2.1) to 773MPa (ST 1.2.2) and, finally, to 742MPa (ST 1.2.3). A larger rate of decrease is observed in the case of elongation to fracture (ε_f), which is decreasing from 61% (ST 1.2.1) to 59% (ST 1.2.2) and, finally, to 46% (ST 1.2.3). The observed decrease must be linked to the induced microstructural changes (see Table 6.7), where one can observe that increasing the solution treatment duration leads to an increase in both the average grain-size and the average weight fraction of the constituent δ-phase (decrease in average weight fraction of the constituent γ phase). No σ-phase was induced during solution treatment at 1050°C.

The microhardness evolution of the δ and γ phases show a continuous increase in microhardness. Overall, it can be observed that the δ phase shows an increase from 269HV0.1 (ST 1.2.1) to 307HV0.1 (ST 1.2.2) and, finally, to 334HV0.1 (ST 1.2.3), while the γ phase from 263HV0.1 (ST 1.2.1) to 292HV0.1 (ST 1.2.2) and, finally, to 354HV0.1 (ST

1.2.3) (see Table 7.4). This kind of behaviour must be linked to the changes in the chemical composition of the constituent δ and γ phases occurring during solution treatment.

In order to explain this behaviour, it should consider the overall influence of the law of mixture (the influence of average weight fraction) and the influence of Hall-Petch relation (the influence of average grain-size) competitive mechanisms. The observed mechanical behaviour, decrease in both strength and ductility properties, suggests that the most influential factor is constituted by the increased average grain-size of the constituent δ and γ phases.

Table 7.4

Mechanical properties of ST 1.2 state.

Structural state / Solution treatment at 1050ºC (ST 1.2)	**Mechanical properties**					
	Microhardness			σ_{UTS} [MPa]	$\sigma_{0.2}$ [MPa]	ε_f [%]
	δ [HV0.1]	**γ** [HV0.1]	**σ+γ2** [HV0.025]			
Solution treated: 1050°C/20mins/WQ (**ST 1.2.1**)	269±14	263±21	-	793±15	480±9	61±2
Solution treated: 1050°C/40mins/WQ (**ST 1.2.2**)	307±16	292±19	-	773±12	496±14	59±2
Solution treated: 1050°C/60mins/WQ (**ST 1.2.3**)	334±22	354±26	-	742±11	432±10	46±3

7.4.3. Solution treatment at 1100°C (ST1.3) state

Table 7.5 presents the obtained mechanical properties after applying a solution treatment at 1100°C (ST 1.3), with a variable treatment duration of 20min (ST 1.3.1), 40min (ST 1.3.2) and 60min (ST 1.3.3), on the hot deformed at 1000°C (HD1) samples. Analysing the effects induced by applying a solution treatment at 1100°C (ST 1.3) with a variable treatment duration of 20min (ST 1.3.1), shows that there was an increase in alloy overall mechanical properties. The ultimate tensile strength (σ_{UTS}) is increasing from 768MPa (HD1 sate) to 787MPa (ST 1.3.1 sate) and the elongation to fracture (ε_f) from 34% (HD1 sate) to 72% (ST 1.3.1 sate), indicating that the newly recrystallized microstructure is completely free of unwanted/deleterious effects induced by the intense plastic deformation. By analysing the influence of increasing the solution treatment duration, from 20min (ST 1.3.1) to 40min (ST 1.3.2) and, finally, to 60min (ST 1.3.3), it can be noticed that an almost identical behaviour with the result of solution treated performed at 1050°C (ST 1.2 state), where both strength and ductility properties are decreasing. Also, it can be noticed that the ultimate tensile strength (σ_{UTS}) was continuously decreased, from 787MPa (ST 1.3.1) to 771MPa (ST 1.3.2) and, finally, to 744MPa (ST 1.3.3). Also, a larger rate of decrease was observed in the case of elongation to fracture (ε_f), from 72% (ST 1.3.1) to 64% (ST 1.3.2) and, finally, to 54% (ST 1.3.3). The observed decrease must be linked to the induced microstructural changes (see Table 6.8), increasing the solution treatment duration leads to an increase in both the average grain-size and the average weight fraction of the constituent δ-phase (decrease in the average weight fraction of the constituent γ-phase). The microhardness evolution of the δ and γ phases, also, shows a continuous increase. Overall, it can be observed that the δ-phase show an increase, from 295HV0.1 (ST 1.3.1) to 286HV0.1 (ST 1.3.2) and, finally, to 339HV0.1 (ST 1.3.3), while the γ-phase shows very minimal variations (almost constant microhardness), from 260HV0.1 (ST 1.3.1) to 266HV0.1 (ST 1.3.2) and, finally, to 264HV0.1 (ST 1.3.3) (see Table 7.5). This result indicates that the changes in the chemical composition of the constituent δ and γ phases are minimal.

Table 7.5

Mechanical properties of ST 1.3 state.

Structural state / Solution treatment at 1100ºC (ST 1.3)	Mechanical properties					
	Microhardness			σ_{UTS} [MPa]	$\sigma_{0.2}$ [MPa]	ε_f [%]
	δ [HV0.1]	γ [HV0.1]	$\sigma+\gamma_2$ [HV0.025]			
Solution treated: 1100°C/20mins/WQ (**ST 1.3.1**)	295±20	260±18	-	787±15	475±11	72±4
Solution treated: 1100°C/40mins/WQ (**ST 1.3.2**)	286±24	266±16	-	771±12	477±7	64±2
Solution treated: 1100°C/60mins/WQ (**ST 1.3.3**)	339±27	264±22	-	744±9	476±12	54±4

7.5. Hot deformation at 1050ºC (HD2) state

Table 7.6 presents the obtained mechanical properties of F55 SDSS alloy due to the hot deformation at 1050°C (HD2). Compared with the AR state, it can observe that the strength properties are showing a small increase, i.e., ultimate tensile strength σ_{UTS} = 826MPa and yield strength $\sigma_{0.2}$ = 540MPa, while the ductility properties, i.e., elongation to fracture ε_f = 50%, are showing a decrease. This behaviour can be explained based on the microstructural changes that occurred during hot deformation. During deformation, the fragmentation of the grains occurs, leading to smaller size grains, grains rotations and a higher / increased defect density, in order to accommodate the applied strain/stress field. As shown in chapter 6.5, it can notice that due to the intensely deformed δ-phase and γ-phase grains, the strain-hardening phenomena occur, leading an increase in strength and decrease in ductility. Also, it must consider the influence of the precipitated deleterious σ-phase, being known that the small-size σ-phase precipitates can act as strengthening particles. As shown in Table 7.6, the microhardness of both constituent δ and γ phases are increasing, to 306HV0.1 and respectively 306HV0.1, due to the strain hardening that occurred during deformation. The microhardness recorded in the case of γ phase small increase proves that the γ-phase grains are more strain hardened, showing a higher defects density compared with the constituent δ phase.

Table 7.6

Mechanical properties of HD2 state.

Structural state	Mechanical properties					
	Microhardness			σ_{UTS} [MPa]	$\sigma_{0.2}$ [MPa]	ε_f [%]
	δ [HV0.1]	γ [HV0.1]	$\sigma+\gamma_2$ [HV0.025]			
Hot-rolled (**HD2**) at 1050°C	306±12	306±14	491±19	826±8	540±12	50±2

As previously shown, this behaviour resides in the crystallography of the FCC γ-phase compared with the BCC δ-phase, which accommodates better the applied strain/stress field by slip/twinning on its higher atomic density planes for the same applied stress/strain level [110-111]. Also, it must consider the presence of precipitated σ-phase, which is forms, eighter by precipitation ($\delta \rightarrow \sigma$) or by eutectoid decomposition ($\delta \rightarrow \sigma + \gamma_2$). As shown in Table 7.6, it can be observed that the global microhardness of the ($\sigma + \gamma_2$) is reaching 491HV0.025.

7.6. Solution treatment (ST2) state

7.6.1. Solution treatment at 1000°C (ST2.1) state

Table 7.7 presents the obtained mechanical properties after applying a solution treatment at 1000°C (ST 2.1), with a variable treatment duration of 20min (ST 2.1.1), 40min (ST 2.1.2)

and 60min (ST 2.1.3), on the hot deformed at 1050°C (HD2) samples. Compared with the HD2 state, it can observe that the strength properties are showing a small decrease in the case of both ultimate tensile strength (σ_{UTS}) and yield strength ($\sigma_{0.2}$) while, in the case of elongation to fracture (ε_f) an increase. The ultimate tensile strength (σ_{UTS}) is continuously decreasing, from 746MPa (ST 2.1.1) to 745MPa (ST 2.1.2) and, finally, to 730MPa (ST 2.1.3) while, the yield strength increases ($\sigma_{0.2}$), from 468MPa to 485MPa and, finally, to 479MPa. The elongation to fracture (ε_f) is, also, continuously decreasing, from 64% (ST 2.1.1) to 61% (ST 2.1.2) and, finally, to 61% (ST 2.1.3) (see Table 7.7).

The microhardness evolution of all δ, γ and ($\sigma+\gamma_2$) constituent phases shows small decreasing, minimal variations are occurring while increasing solution treatment duration, all values being within the dispersion variation (see Table 7.7). Overall, it can be observed that the δ phase shows a microhardness varying within 284HV0.1 to 309HV0.1 range, γ phase showing a smaller microhardness compared with the δ phase, within 243HV0.1 to 253HV0.1 range and, ($\sigma+\gamma_2$) microhardness within 513HV0.025 to 527HV0.025 range.

Table 7.7

Mechanical properties of ST 2.1 state.

Structural state / Solution treatment at 1000ºC (ST 2.1)	**Mechanical properties**					
	Microhardness			**σ_{UTS}** [MPa]	**$\sigma_{0.2}$** [MPa]	**ε_f** [%]
	δ [HV0.1]	**γ** [HV0.1]	**$\sigma+\gamma_2$** [HV0.025]			
Solution treated: 1000°C/20mins/WQ (**ST 2.1.1**)	309±16	253±24	527±21	746±10	468±14	64±2
Solution treated: 1000°C/40mins/WQ (**ST 2.1.2**)	292±22	250±23	523±24	745±7	485±8	61±3
Solution treated: 1000°C/60mins/WQ (**ST 2.1.3**)	284±25	243±18	513±18	730±11	479±11	61±3

This observed mechanical behaviour must be explained considering the occurred microstructural changes during applied solution treatment. The explanation must consider the following competing mechanisms, firstly, the law of phase mixture of constituent phases and, secondly, the Hall-Pech grain-size influence. According to the law of phase mixture states, the exhibited properties are proportionally influenced by the weight fraction of a particular phase [114]. Considering the specific case of the SDSS alloys, it was shown that the γ phase is responsible for the plasticity/ductility while the δ-phase is responsible for the strength properties [108]. Also, it was shown that the precipitation of the σ-phase influenced all exhibited mechanical properties by inducing embrittlement [115]. As shown in chapter 6.6.1, it can notice that due to the applied solution treatment, besides both δ and γ phases the deleterious σ phase was induced too. Also, it can be noticed that the wight fraction of the σ phase is increasing with treatment duration increasing from 1.1wt% (ST 2.1.1) to 1.7wt% (ST 2.1.2) and, finally, to 2.9wt% (ST 2.1.3), diminishing all exhibited mechanical properties (strength/ductility) (see Table 7.7).

As shown in chapter 6.6.1 (see Table 6.10), it can notice that small variations in the average grain-size of the constituent phases are occurring during solution treatment (ST 2.1). Analysing the case of the δ-phase, it can be observed a small increase from 57.2μm (ST 2.1.1) to 69.2μm (ST 2.1.2) and, finally, to 74.5μm (ST 2.1.3), from 19.1μm (ST 2.1.1) to 24.4μm (ST 2.1.2) and, finally, to 29.5μm (ST 2.1.3) in the case of γ phase and, from 5.3μm (ST 2.1.1) to 7.2μm (ST 2.1.2) and, finally, to 8.2μm (ST 2.1.3) in the case of σ phase. According to the Hall-Pech relation, those small increases in the average grain-sizes of the

constituent phases will lead to an overall decrease in the alloy's strength and ductility properties (see Table 7.7).

7.6.2. Solution treatment at 1050°C (ST2.2) state

Table 7.8 presents the obtained mechanical properties after applying a solution treatment at 1050°C (ST 2.2), with a variable treatment duration of 20min (ST 2.2.1), 40min (ST 2.2.2) and 60min (ST 2.2.3), on hot deformation at 1050°C (HD2) samples.

Analysing the effects induced by applying a solution treatment at 1050°C (ST 2.2) with a variable treatment duration of 20min (ST 2.2.1), can be noticed an increase in alloy overall mechanical properties. The ultimate tensile strength (σ_{UTS}) is decreasing, from 826MPa (HD2 state) to 793MPa (ST 2.2.1 state) and, the elongation to fracture(ε_f) increased, from 50% (HD2 state) to 61% (ST 2.2.1 sate), indicating that the newly recrystallized microstructure has removed the unwanted/deleterious effects induced by the intense plastic deformation. Analysing the influence of increasing the solution treatment duration from 20min (ST 2.2.1) to 40min (ST 2.2.2) and, finally, to 60min (ST 2.2.3), it can be noticed that both strength and ductility properties are decreasing. It can be observed that the ultimate tensile strength (σ_{UTS}) is continuously decreasing, from 793MPa (ST 2.2.1) to 773MPa (ST 2.2.2) and, finally, to 742MPa (ST 2.2.3). A larger rate of decrease is observed in the case of elongation to fracture (ε_f), which is decreasing, from 61% (ST 2.2.1) to 59% (ST 2.2.2) and, finally, to 46% (ST 2.2.3). The observed decrease must be linked to the induced microstructural changes (see Table 6.11), where one can observe that increasing the solution treatment duration leads to an increase in both the average grain-size and the average weight fraction of constituent δ-phase (decrease in the average weight fraction of the constituent γ-phase). No σ-phase was induced during solution treatment at 1050°C.

The microhardness evolution of δ and γ phases show a continuous increase. Overall, it can be observed that the δ-phase shows an increase, from 269HV0.1 (ST 2.2.1) to 307HV0.1 (ST 2.2.2) and, finally, to 334HV0.1 (ST 2.2.3), while the γ-phase, from 263HV0.1 (ST 2.2.1) to 292HV0.1 (ST 2.2.2) and, finally, to 354HV0.1 (ST 2.2.3) (see Table 7.8). This kind of behaviour must be linked to the changes in the chemical composition of the constituent δ and γ phases occurring during solution treatment.

Table 6.8

Mechanical properties of ST 2.2 state.

Structural state / Solution treatment at 1050ºC (ST 2.2)	**Mechanical properties**					
	Microhardness			**σ_{UTS}** [MPa]	**$\sigma_{0.2}$** [MPa]	**ε_f** [%]
	δ [HV0.1]	**γ** [HV0.1]	**σ+γ₂** [HV0.025]			
Solution treated: 1050°C/20mins/WQ (**ST 2.2.1**)	269±19	263±13	-	793±8	480±13	61±3
Solution treated: 1050°C/40mins/WQ (**ST 2.2.2**)	307±14	292±27	-	773±14	496±10	59±3
Solution treated: 1050°C/60mins/WQ (**ST 2.2.3**)	334±19	354±24	-	742±14	432±11	46±2

7.6.3. Solution treatment at 1100°C (ST2.3) state

Table 7.9 presents the obtained mechanical properties after applying a solution treatment at 1100°C (ST 2.3), with a variable treatment duration of 20min (ST 2.3.1), 40min (ST 2.3.2) and 60min (ST 2.3.3), on hot deformed at 1050°C (HD2) samples. Analysing the effects induced by applying a solution treatment at 1100°C (ST 2.3) with a variable treatment duration of 20min (ST 2.3.1) it can be noticed that an increase in alloy overall mechanical properties is obtained. The ultimate tensile strength (σ_{UTS}) is decreasing, from 826MPa (HD2

sate) to 782MPa (ST 2.3.1 sate) and, the elongation to fracture (ε_f) from 50% (HD2 sate) to 61% (ST 2.3.1 sate), indicating that the newly recrystallized microstructure is completely free of unwanted/ deleterious effects induced by the intense applied deformation.

Analysing the influence of increasing the solution treatment duration from 20min (ST 2.3.1) to 40min (ST 2.3.2) and, finally, to 60min (ST 2.3.3), can be seen an almost identical behaviour to the one observed in the case of solution treatment performed at 1050°C (ST 2.2 state), where both strength and ductility properties are decreasing. It can be observed that the ultimate tensile strength (σ_{UTS}) is continuously decreasing, from 782MPa (ST 2.3.1) to 743MPa (ST 2.3.2) and, finally, to 776MPa (ST 2.3.3). Also, a larger rate of decrease is observed in the case of elongation to fracture (ε_f), which is decreasing from 61% (ST 2.3.1) to 59% (ST 2.3.2) and, finally, to 54% (ST 2.3.3). The observed decrease must be linked to the induced microstructural changes (see Table 6.11), where one can observe that increasing the solution treatment duration leads to an increase in both the average grain-size and the average weight fraction of constituent δ-phase (decrease in the average weight fraction of the constituent γ-phase).

Table 7.9

Mechanical properties of ST 2.3 state.

Structural state / Solution treatment at 1100ºC (ST 2.3)	**Mechanical properties**					
	Microhardness			**σ_{UTS}** [MPa]	**$\sigma_{0.2}$** [MPa]	**ε_f** [%]
	δ [HV0.1]	**γ** [HV0.1]	**σ+γ2** [HV0.025]			
Solution treated: 1100°C/20mins/WQ (**ST 2.3.1**)	308±21	266±15	-	782±11	458±13	61±4
Solution treated: 1100°C/40mins/WQ (**ST 2.3.2**)	338±14	249±18	-	743±14	463±11	59±3
Solution treated: 1100°C/60mins/WQ (**ST 2.3.3**)	351±17	248±22	-	776±16	478±11	54±4

The microhardness evolution of the δ and γ phases, also, shows a continuous increase in microhardness. Overall, it can be observed that the δ-phase shows an increase, from 308HV0.1 (ST 2.3.1) to 338HV0.1 (ST 2.3.2) and, finally, to 358HV0.1 (ST 2.3.3), while the γ-phase shows very minimal variations (almost constant microhardness), from 266HV0.1 (ST 2.3.1) to 249HV0.1 (ST 2.3.2) and, finally, to 248HV0.1 (ST 2.3.3) (see Table 7.9), indicating that the changes in the chemical composition of the constituent δ and γ phases are minimal.

7.7. Hot deformation at 1100ºC (HD3) state

Table 7.10 presents the obtained mechanical properties of F55 SDSS alloy due to the hot deformation at 1100°C (HD3). Compared with the AR state, it can observe that the strength properties are showing a small increase, i.e., ultimate tensile strength σ_{UTS} = 804MPa and yield strength $\sigma_{0.2}$ = 431MPa, while the ductility properties, i.e., elongation to fracture ε_f = 45%, are showing a decrease. This behaviour can be explained based on the microstructural changes that occurred during hot deformation. During deformation the fragmentation of the grains occurs, leading to smaller size grains, grains rotations and a higher / increased defect density to accommodate the applied strain/stress field. As shown in section 6.7, it can be noticed that due to the intensely deformed δ-phase and γ-phase grains, the strain-hardening phenomena occur, leading to an increase in strength and decrease in ductility. Also, the ultimate tensile strength σ_{UTS} is smaller in comparison with the HD2 case due to the no deleterious σ-phase precipitation.

Table 7.10

Mechanical properties of HD3 state.

Structural state	Mechanical properties					
	Microhardness			σ_{UTS} [MPa]	$\sigma_{0.2}$ [MPa]	ε_f [%]
	δ [HV0.1]	**γ** [HV0.1]	**σ+γ₂** [HV0.025]			
Hot-rolled (**HD3**) at 1100°C	321±8	280±14	-	804±7	431±12	45±3

As shown in Table 7.10, it can be observed that the microhardness of the δ-phase and γ-phase is increasing, to 321HV0.1 and 280HV0.1 respectively, due to the strain hardening that occurred during deformation. The microhardness recorded in the case of the γ-phase shows a small increase, proving that the γ-phase grains are more strain hardened.

7.8. Solution treatment (ST3) state

7.8.1. Solution treatment at 1000°C (ST3.1) state

Table 7.11 presents the obtained mechanical properties after applying a solution treatment at 1000°C (ST 3.1), with a variable treatment duration of 20min (ST 3.1.1), 40min (ST 3.1.2) and 60min (ST 3.1.3), on the hot deformed at 1100°C (HD3) samples. Compared with the HD3 state, it can be observed that both strength properties (ultimate tensile strength (σ_{UTS}) and yield strength ($\sigma_{0.2}$)) are showing a decrease while in the case of elongation to fracture (ε_f) an increase. The ultimate tensile strength (σ_{UTS}) is continuously increasing, from 762MPa (ST 3.1.1) to 764MPa (ST 3.1.2) and, finally, to 673MPa (ST 3.1.3), while the yield strength is increasing ($\sigma_{0.2}$) from, 410MPa to 420MPa and, finally, to 423MPa. The elongation to fracture (ε_f) is continuously decreasing, from 66% (ST 3.1.1) to 46% (ST 3.1.2) and, finally, to 37% (ST 3.1.3) (see Table 6.11).

Table 7.11

Mechanical properties of ST 3.1 state.

Structural state / Solution treatment at 1000ºC (ST 3.1)	Mechanical properties					
	Microhardness			σ_{UTS} [MPa]	$\sigma_{0.2}$ [MPa]	ε_f [%]
	δ [HV0.1]	**γ** [HV0.1]	**σ+γ₂** [HV0.025]			
Solution treated: 1000°C/20mins/WQ (**ST 3.1.1**)	295±11	257±16	507±29	762±7	410±12	66±4
Solution treated: 1000°C/40mins/WQ (**ST 3.1.2**)	297±18	257±17	516±28	764±14	420±8	46±4
Solution treated: 1000°C/60mins/WQ (**ST 3.1.3**)	282±19	260±14	513±21	673±12	423±9	37±4

The microhardness evolution of all δ, γ and (σ+γ₂) constituent phases shows that the microhardness shows minimal variations while increasing the solution treatment duration, all values being within the dispersion variation (see Table 7.11). Overall, can be observed that the δ-phase shows a microhardness varying within 282HV0.1 to 297HV0.1 range, γ-phase varying within 257HV0.1 to 260HV0.1 range and, (σ+γ₂) microhardness within 507 HV0.025 to 516 HV0.025 range.

This observed mechanical behaviour must be explained by considering the occurred microstructural changes during applied solution treatment. The explanation must consider the following competing mechanisms, firstly, the law of phase mixture of constituent phases and, secondly, the Hall-Pech grain-size influence. As shown in section 6.8.1, it can be noticed that due to the applied solution treatment, besides both δ and γ phases the deleterious σ phase is induced too. Also, it can notice that the wight fraction of the σ-phase is increasing with

treatment duration increasing from 2.9wt% (ST 3.1.1) to 4.5wt% (ST 3.1.2) and, finally, to 7.5wt% (ST 3.1.3), diminishing all exhibited mechanical properties (strength/ductility) (see Table 7.11).

As shown in section 6.8.1 (see Table 6.14), it can be seen that small variations in the average grain-size of constituent phases are occurring during solution treatment (ST 3.1). Analysing the case of the δ-phase, it can be observed a small increase, from 40.2μm (ST 3.1.1) to 58.6μm (ST 3.1.2) and, finally, to 55.7μm (ST 3.1.3), from 26.1μm (ST 3.1.1) to 22.7μm (ST 3.1.2) and, finally, to 19.1μm (ST 3.1.3) in the case of γ phase and, from 4.7μm (ST 3.1.1) to 6.8μm (ST 3.1.2) and, finally, to 7.1μm (ST 3.1.3) in the case of σ phase. According to the Hall-Pech relation, those small increases in the average grain-sizes of the constituent phases will lead to an overall decrease in alloy's strength and ductility properties (see Table 7.11).

7.8.2. Solution treatment at 1050°C (ST3.2) state

Table 7.12 presents the obtained mechanical properties after applying a solution treatment at 1050°C (ST 3.2), with a variable treatment duration of 20min (ST 3.2.1), 40min (ST 3.2.2) and 60min (ST 3.2.3), on the hot deformed at 1100°C (HD3) samples. Analysing the effects induced by applying a solution treatment at 1050°C (ST 3.2) with a variable treatment duration of 20min (ST 3.2.1), it can be noticed that an increase in alloy overall mechanical properties. The ultimate tensile strength (σ_{UTS}) is decreasing, from 804MPa (HD3 state) to 764MPa (ST 3.2.1 state) and the elongation to fracture(ε_f), from 45% (HD3 state) to 65% (ST 3.2.1 state), indicating that the newly recrystallized microstructure has removed the unwanted/deleterious effects induced by the intense applied deformation.

Analysing the influence of increasing the solution treatment duration from 20min (ST 3.2.1) to 40min (ST 3.2.2) and, finally, to 60min (ST 3.2.3), it can be seen that both strength and ductility properties are decreasing. Also, It can be observed that the ultimate tensile strength (σ_{UTS}) is continuously decreasing, from 764MPa (ST 3.2.1) to 760MPa (ST 3.2.2) and, finally, to 738MPa (ST 3.2.3). A smaller rate of decrease is observed in the case of elongation to fracture (ε_f), which is decreasing, from 65% (ST 3.2.1) to 63% (ST 3.2.2) and, finally, to 62% (ST 3.2.3). The observed decrease must be linked to the induced microstructural changes (see Table 6.15), which indicates that increasing the solution treatment duration leads to an increase in the average grain-size and the average weight fraction of constituent δ-phase (decrease in average weight fraction of the constituent γ-phase). No σ-phase was induced during solution treatment at 1050°C.

Table 7.12

Mechanical properties of ST 3.2 state.

Structural state / Solution treatment at 1050ºC (ST 3.2)	**Mechanical properties**					
	Microhardness			**σ_{UTS}** [MPa]	**$\sigma_{0.2}$** [MPa]	**ε_f** [%]
	δ [HV0.1]	**γ** [HV0.1]	**σ+γ2** [HV0.025]			
Solution treated: 1050°C/20mins/WQ (**ST 3.2.1**)	254±14	248±20	-	764±14	439±11	65±4
Solution treated: 1050°C/40mins/WQ (**ST 3.2.2**)	303±13	248±19	-	760±12	430±14	63±3
Solution treated: 1050°C/60mins/WQ (**ST 3.2.3**)	327±11	252±11	-	738±10	419±11	62±3

The microhardness evolution of the δ and γ phases show a continuous increase in microhardness. Overall, it can be observed that the δ-phase shows an increase, from 254HV0.1 (ST 3.2.1) to 303HV0.1 (ST 3.2.2) and, finally, to 327HV0.1 (ST 3.2.3), while the γ-phase, from 248HV0.1 (ST 3.2.1) to 248HV0.1 (ST 3.2.2) and, finally, to 352HV0.1 (ST 3.2.3) (see Table 7.12). This kind of behaviour must be linked to the changes in the chemical composition of the constituent δ and γ phases occurring during solution treatment

7.8.3. Solution treatment at 1100°C (ST3.3) state

Table 7.13 presents the obtained mechanical properties after applying a solution treatment at 1100°C (ST 3.3), with a variable treatment duration of 20min (ST 3.3.1), 40min (ST 3.3.2) and 60min (ST 3.3.3), on the hot deformed at 1100°C (HD3) samples. Analysing the effects induced by applying a solution treatment at 1100°C (ST 3.3) with a variable treatment duration of 20min (ST 3.3.1), it can notice that an increase in alloy overall mechanical properties is obtained. The ultimate tensile strength (σ_{UTS}) is decreasing, from 804MPa (HD3 sate) to 776MPa (ST 3.3.1 sate) and the elongation to fracture (ε_f) is increasing, from 45% (HD3 sate) to 62%, indicating that the newly recrystallized microstructure is completely free of unwanted/deleterious effects induced by the intense plastic deformation.

Table 7.13

Mechanical properties of ST 3.3 state.

Structural state / Solution treatment at 1100ºC (ST 3.3)	**Mechanical properties**					
	Microhardness			**σ_{UTS}** [MPa]	**$\sigma_{0.2}$** [MPa]	**ε_f** [%]
	δ [HV0.1]	**γ** [HV0.1]	**σ+γ2** [HV0.025]			
Solution treated: 1100°C/20mins/WQ (**ST 3.3.1**)	289±11	250±13	-	776±13	380±14	62±2
Solution treated: 1100°C/40mins/WQ (**ST 3.3.2**)	307±18	248±19	-	770±16	351±13	61±2
Solution treated: 1100°C/60mins/WQ (**ST 3.3.3**)	358±22	252±15	-	759±11	345±8	60±3

Analysing the influence of increasing the solution treatment duration from 20min (ST 3.3.1) to 40min (ST 3.3.2) and, finally, to 60min (ST 3.3.3), show that both strengths and ductility are decreasing. It can observe that the ultimate tensile strength (σ_{UTS}) is continuously decreasing, from 776MPa (ST 3.3.1) to 770MPa (ST 3.3.2) and, finally, to 759MPa (ST 3.3.3). A small rate of decrease is observed in the case of elongation to fracture (ε_f), which is decreasing from 62% (ST 3.3.1) to 61% (ST 3.3.2) and, finally, to 60% (ST 3.3.3). The observed decrease must be linked to the induced microstructural changes (see Table 6.16), where one can observe that increasing the solution treatment duration leads to an increase in both the average grain-size and the average weight fraction of constituent δ-phase (decrease in average weight fraction of the constituent γ-phase).

The microhardness evolution of δ and γ phases shows an increase in the case of δ phase while γ is almost constant. Overall, it can be observed that the δ phase shows an increase, from 289 HV0.1 (ST 3.3.1) to 307 HV0.1 (ST 3.3.2) and, finally, to 358 HV0.1 (ST 3.3.3), while the γ phase shows very minimal variations (almost constant microhardness) from 250 HV0.1 (ST 3.3.1) to 248 HV0.1 (ST 3.3.2) and, finally, to 252 HV0.1 (ST 3.3.3) (see Table 7.13), indicating that the changes in the chemical composition of the constituent δ and γ phases are minimal.

7.9. Hot deformation at 1150ºC (HD4) state

Table 7.14 presents the obtained mechanical properties of F55 SDSS alloy due to the hot deformation at 1150°C (HD4). Compared with the AR state, it can observe that the strength

properties are showing a small increase, i.e., ultimate tensile strength σ_{UTS} = 765MPa and yield strength $\sigma_{0.2}$ = 391MPa, while the ductility properties, i.e., elongation to fracture ε_f = 43%, are showing a decrease. This behaviour can be explained based on the microstructural changes that occurred during intense hot deformation. During deformation, the fragmentation of the grains occurs, leading to smaller size grains, grain rotations and a higher/increased defect density to accommodate the applied strain/stress field. As shown in section 6.17, it can be noticed that due to the intensely deformed δ-phase and γ-phase grains, the strain-hardening phenomena occur, leading to an increase in strength and decrease in ductility.

Table 7.14

Mechanical properties of HD4 state.

Structural state	Mechanical properties					
	Microhardness			σ_{UTS} [MPa]	$\sigma_{0.2}$ [MPa]	ε_f [%]
	δ [HV0.1]	γ [HV0.1]	σ+γ2 [HV0.025]			
Hot-rolled (**HD4**) at 1150°C	291±11	304±8	-	765±12	391±9	43±2

7.10. Solution treatment (ST4) state

7.10.1. Solution treatment at 1000°C (ST4.1) state

Table 7.15 presents the obtained mechanical properties after applying a solution treatment at 1000°C (ST 4.1), with a variable treatment duration of 20min (ST 4.1.1), 40min (ST 4.1.2) and 60min (ST 4.1.3), on the hot deformed at 1150°C (HD4) samples. Compared with the HD4 state, it can be observed that the strength properties are showing a decrease while in the case of elongation to fracture (ε_f) an increase. The ultimate tensile strength (σ_{UTS}) is continuously decreasing, from 756MPa (ST 4.1.1) to 740MPa (ST 4.1.2) and, finally, to 737MPa (ST 4.1.3), while the yield strength ($\sigma_{0.2}$), from 310Mpa (ST 4.1.1) to 313Mpa (ST 4.1.2) and, finally, to 308Mpa (ST 4.1.3). The elongation to fracture (ε_f) is, also, continuously high decreasing from 52% (ST 4.1.1) to 47% (ST 4.1.2) and, finally, to 44% (ST 4.1.3) (see Table 7.15).

Table 7.15

Mechanical properties of ST 4.1 state.

Structural state / Solution treatment at 1000ºC (ST 4.1)	Mechanical properties					
	Microhardness			σ_{UTS} [MPa]	$\sigma_{0.2}$ [MPa]	ε_f [%]
	δ [HV0.1]	γ [HV0.1]	σ+γ2 [HV0.025]			
Solution treated: 1000°C/20mins/WQ (**ST 4.1.1**)	299±10	249±11	525±27	756±14	310±8	52±4
Solution treated: 1000°C/40mins/WQ (**ST 4.1.2**)	287±11	246±14	519±20	740±13	313±10	47±3
Solution treated: 1000°C/60mins/WQ (**ST 4.1.3**)	292±13	239±10	518±28	737±13	308±14	44±4

The microhardness evolution of all δ, γ and (σ+γ2) constituent phases shows minimal variations, all values being within the dispersion variation (see Table 7.15). Overall, it can be observed that the δ-phase shows a microhardness varying within 287HV0.1 to 299HV0.1 range, γ-phase varying within 239HV0.1 to 249HV0.1 range and, (σ+γ2) varying within 518HV0.025 to 525 HV0.025 range.

As shown in chapter 6.10.1 (see Table 6.18), it can be noticed that small variations in the average grain-size of constituent phases are occurring during solution treatment (ST 4.1). Analysing the case of the δ-phase, it can be observed a small increase from 45.5μm (ST

4.1.1) to 34.4μm (ST 4.1.2) and, finally, to 28.7μm (ST 4.1.3), from 30.9μm (ST 4.1.1) to 24.6μm (ST 4.1.2) and, finally, to 19.9μm (ST 4.1.3) in the case of γ-phase and, from 4.4μm (ST 4.1.1) to 5.2μm (ST 4.1.2) and, finally, to 6.2μm (ST 4.1.3) in the case of σ-phase. According to the Hall-Pech relation, those small increases in the average grain-sizes of the constituent phases will lead to an overall decrease in the alloy's strength and ductility properties (see Table 7.15).

6.10.2. Solution treatment at 1050°C (ST4.2) state

Table 7.16 presents the obtained mechanical properties after applying a solution treatment at 1050°C (ST 4.2), with a variable treatment duration of 20min (ST 4.2.1), 40min (ST 4.2.2) and 60min (ST 4.2.3), on the hot deformed at 1150°C (HD4) samples. Comparing the hot deformed at 1150°C (HD4) state with the solution treated at 1050°C with a treatment duration of 20min (ST 4.2.1) state can be observed that the ultimate tensile strength (σ_{UTS}) is decreasing, from 765MPa (HD4 state) to 735MPa (ST 4.2.1 state) while the elongation to fracture (ε_f) is increased, from 43% (HD4 state) to 80% (ST 4.2.1 state), indicating that the newly recrystallized microstructure has removed the unwanted/deleterious effects induced by the intense deformation.

Table 7.16

Mechanical properties of ST 4.2 state.

Structural state / Solution treatment at 1050ºC (ST 4.2)	**Mechanical properties**					
	Microhardness			**σ_{UTS}** [MPa]	**$\sigma_{0.2}$** [MPa]	**ε_f** [%]
	δ [HV0.1]	**γ** [HV0.1]	**σ+γ2** [HV0.025]			
Solution treated: 1050°C/20mins/WQ (**ST 4.2.1**)	277±9	246±16	-	735±7	405±10	80±5
Solution treated: 1050°C/40mins/WQ (**ST 4.2.2**)	290±10	244±17	-	737±10	406±12	77±4
Solution treated: 1050°C/60mins/WQ (**ST 4.2.3**)	301±12	243±12	-	754±11	406±12	70±4

Analysing the influence of increasing the solution treatment duration from 20min (ST 4.2.1) to 40min (ST 4.2.2) and, finally, to 60min (ST 4.2.3), it can be seen that ductility property is decreasing while strength properties are increasing. Also, It can be observed that the ultimate tensile strength (σ_{UTS}) is continuously increasing, from 735MPa (ST 4.2.1) to 737MPa (ST 4.2.2) and, finally, to 754MPa (ST 4.2.3). A smaller rate of decrease is observed in the case of elongation to fracture (ε_f) which is decreasing, from 80% (ST 4.2.1) to 77% (ST 4.2.2) and, finally, to 70% (ST 4.2.3). The observed decrease must be linked to the induced microstructural changes (see Table 6.18), where one can observe that increasing the solution treatment duration leads to a decrease in both the average grain-size and the average weight fraction of the constituent δ-phase, while the average weight fraction of γ-phase was increased. There is no σ-phase induced during solution treatment at 1050°C. The microhardness evolution of the δ-phase shows a continuous increase in the microhardness while the microhardness of the γ-phase is almost constant. Overall, it can be observed that the δ-phase shows an increase, from 277HV0.1 (ST 4.2.1) to 299 HV0.1 (ST 4.2.2) and, finally, to 301 HV0.1 (ST 4.2.3), while the γ-phase from 246HV0.1 (ST 4.2.1) to 244 HV0.1 (ST 4.2.2) and, finally, to 243HV0.1 (ST 4.2.3) (see Table 7.16). This kind of behaviour must be linked to the changes in the chemical composition of the constituent δ and γ phases occurring during solution treatment.

7.10.3. Solution treatment at 1100°C (ST4.3) state

Table 7.17 presents the obtained mechanical properties after applying a solution treatment at 1100°C (ST 4.3), with a variable treatment duration of 20min (ST 4.3.1), 40min (ST 4.3.2) and 60min (ST 4.3.3), on the hot deformed at 1150°C (HD4) samples. Analysing the effects induced by applying a solution treatment at 1100°C (ST 4.3) with a variable treatment duration of 20min (ST 4.3.1), it can notice that an increase in alloy overall mechanical properties is obtained. The ultimate tensile strength (σ_{UTS}) is increasing from 765MPa (HD4 state) to 769MPa (ST 4.3.1 state) while the elongation to fracture (ε_f) is increasing from 43% (HD4 state) to 69% (ST 4.3.1 state), indicating that the newly recrystallized microstructure is completely free of unwanted/deleterious effects induced by the intense deformation.

Analysing the influence of increasing the solution treatment duration from 20min (ST 4.3.1) to 40min (ST 4.3.2) and, finally, to 60min (ST 4.3.3), show that both strength and ductility properties are decreasing. It can be observed that the ultimate tensile strength (σ_{UTS}) is continuously decreasing, from 769MPa (ST 3.3.1) to 758MPa (ST 4.3.2) and, finally, to 746MPa (ST 4.3.3). A small rate of decrease is observed in the case of elongation to fracture (ε_f), which is decreasing, from 69% (ST 4.3.1) to 65% (ST 4.3.2) and, finally, to 62% (ST 4.3.3). The observed decrease must be linked to the induced microstructural changes (see Table 6.20), where one can observe that increasing the solution treatment duration leads to an increase in both the average grain-size and the average weight fraction of constituent δ-phase (decrease in average weight fraction of the constituent γ-phase).

Table 6.17

Mechanical properties of ST 4.3 state.

Structural state / Solution treatment at 1100ºC (ST 4.3)	**Mechanical properties**					
	Microhardness			**σ_{UTS}** [MPa]	**$\sigma_{0.2}$** [MPa]	**ε_f** [%]
	δ [HV0.1]	**γ** [HV0.1]	**σ+γ₂** [HV0.025]			
Solution treated: 1100°C/20mins/WQ (**ST 4.3.1**)	311±15	241±11	-	769±11	406±11	69±4
Solution treated: 1100°C/40mins/WQ (**ST 4.3.2**)	311±10	255±10	-	758±16	402±12	65±2
Solution treated: 1100°C/60mins/WQ (**ST 4.3.3**)	354±17	265±11	-	746±12	404±9	62±3

The microhardness evolution of δ and γ phases, also, shows a continuous increase. Overall, it can be observed that the δ-phase shows an increase, from 311 HV0.1 (ST 4.3.1) to 311 HV0.1 (ST 4.3.2) and, finally, to 354 HV0.1 (ST 4.3.3), while the γ-phase, from 241 HV0.1 (ST 4.3.1) to 255HV0.1 (ST 4.3.2) and, finally, to 265 HV0.1 (ST 4.3.3) (see Table 7.17), indicating that the changes in the chemical composition of the constituent δ and γ phases are minimal.

7.11. Conclusions

The following conclusions arise from the advanced analysis of the F55 SDSS alloy mechanical properties evolution during thermomechanical processing:

- The ferrite (δ) phase is responsible for the strength properties, the austenite (γ) phase for ductility properties, while the sigma (σ) phase induces embrittlement; the mechanical behaviour is governed by the following competing mechanisms, firstly, the law of constituent phase mixture and, secondly, the Hall-Pech grain-size influence; the average grain-size and the weight fraction of the microstructural constituents (austenite

γ-phase, ferrite δ-phase and sigma σ-phases), are influencing the exhibited mechanical behaviour;

- Generally, for a solution treatment temperature assuring precipitation of the sigma (σ) phase, it can be observed a significant deterioration of the ductility properties (i.e. elongation to fracture) in comparison with the strength properties, due to the induced embrittlement, even for small precipitated weight fractions; i.e. in the case of samples hot deformed at 1100°C (HD 3) and solution treated at 1000°C with a treatment duration from 20min (ST 3.1.1) to 60min (ST 3.1.1) it was noticed a significant decrease in the elongation to fracture, from 66% (ST 3.1.1) to 37% (ST 3.1.3), while the ultimate tensile strength showed a smaller decrease, from 762MPa (ST 3.1.1) to 673MPa (ST 3.1.3);
- Generally, for a solution treatment temperature above the necessary threshold to assure the precipitation of the sigma (σ) phase, it can be observed that the strength and ductility properties are strictly related to the law of constituent phase mixture and the Hall-Pech grain-size influence; the best combination of mechanical properties, high-strength – high ductility, is obtained for a solution treatment performed just above the sigma (σ) precipitation threshold (1050°C); i.e. an ultimate tensile strength close 793Mpa, elongation to fracture close to 61%, were recorded in the case of HD 1 + ST 1.1.1, respectively 793MPa and 61% in the case of HD 2 + ST 2.1.1, respectively 764MPa and 65% in the case of HD 3 + ST 3.1.1 and, respectively 735MPa and 80% in the case of HD 4 + ST 4.1.1;
- In order to control the alloy's mechanical behaviour and to obtain a suitable combination of strength-ductility properties, one must control the morphology, grain-size and weight fraction of the alloy's constituent phases.

Chapter 8: General conclusions, personal contributions, recommendations and future research directions

8.1. General conclusions

The thesis deals centrally with the investigation of the influence of the thermomechanical processing parameters/conditions upon the developed/induced microstructure and mechanical behaviour in the case of S32760 / F55 Super Duplex Stainless Steel (SDSS) alloy. As a key influence parameter in the thermomechanical processing route, the thesis considers the generation/precipitation of the deleterious σ-phase, which plays a key role in both the microstructure and the mechanical behaviour.

The following key general conclusions are emerging from the thesis:

- During mechanical processing, by hot rolling, increasing the deformation temperature, from 1000°C (HD 1) to 1150°C (HD 4), leads to an increase in the defect's density in both the austenite (γ) and the ferrite (δ) phases.
- During mechanical processing, by hot rolling, increasing the deformation temperature, from 1000°C (HD 1) to 1150°C (HD 4), leads to an increase in the average weight fraction of ferrite (δ) phase, from 45.8wt% (HD 1) to 59.3wt% (HD 4) and decrease in the average weight fraction of austenite (γ) phase, from 50.7wt% (HD 1) to 40.7wt% (HD 4), due to the increase kinetics of the $\gamma \rightarrow \delta$ phase transition.

- The σ-phase was precipitated in the microstructure during mechanical processing, by hot rolling, at deformation temperatures below 1000°C. The σ-phase induces embrittlement, with a detrimental effect on the alloy's mechanical behaviour. *Therefore, the hot deformation temperature must be higher than 1000°C, ideal above 1050°C, to prevent the generation/precipitation of the σ-phase within the S32760 / F55 alloy microstructure.*
- Applying a solution treatment, from 1000°C to 1100°C, after hot deformation leads to regeneration of both parent austenite (γ) and ferrite (δ) phases, all showing a low density of defects, no in-grain rotations/deflections and low residual strain-stress fields.
- The σ-phase was precipitated in the microstructure, during thermal processing by solution treatment, at treatment temperatures below 1000°C (ST1.1, ST2.1, ST3.1 and ST4.1 states) and, its weight-fraction increases with the increase in the solution treatment duration, the highest amount being obtained in all cases for the solution treatment performed with a treatment duration of 60min: ST1.1.3 ~ 5.5%wt; ST2.1.3 ~ 2.9%wt; ST3.1.3 ~ 7.4%wt; ST4.1.3 ~ 5.5%wt. *Therefore, the thermal processing by solution treatment must be performed at a treatment temperature higher than 1000°C, ideal above 1050°C, to prevent the generation/precipitation of the σ-phase within the S32760 / F55 alloy microstructure.*
- The σ-phase can be generated as follows:
    - at δ / γ grain boundaries, within the δ-phase grains, by δ → σ precipitation.
    - at δ / δ grain boundaries, within the δ-phase grains, by δ → σ + γ_2 eutectoid decomposition / precipitation.
- An increase in the solution treatment temperature, from 1000°C to 1100°C, leads to an increase in average grain-size of both austenite (γ) and ferrite (δ) phases; the highest values being recorded in the case of samples hot deformed at 1150°C (HD 4) and solution treated at 1100°C for 60min (ST 4.3.3) when the average grain-size of the austenite was close to 40.6μm and the average grain-size of the ferrite was close to 112μm;
- An increase in the solution treatment temperature, from 1000°C to 1100°C, leads to an increase in the average weight fraction of the ferrite (δ) phase and a decrease in the average weight fraction of the austenite (γ) phase; the highest average weight fraction of the ferrite phase being recorded in the case of samples hot deformed at 1150°C (HD 4) and solution treated at 1100°C for 60min (ST 4.3.3) - close to 66.7wt%, while the average weight fraction of the austenite phase - close to 33.3wt%;
- Annealing twins are formed within the austenite (γ) phase during solution treatment.
- The ferrite (δ) phase is responsible for the strength properties, the austenite (γ) phase for ductility properties, while the sigma (σ) phase induces embrittlement; the mechanical behaviour is governed by the following competing mechanisms, firstly, the law of phase mixture of constituent phases and, secondly, the Hall-Pech grain-size influence; the average grain-size and weight fraction of the microstructural constituents, austenite (γ), ferrite (δ) and sigma (σ) phases, are influencing the mechanical behaviour the F55 alloy.
- Generally, for a solution treatment temperature assuring precipitation of the sigma (σ) phase can be observed a significant deterioration of ductility properties (i.e. elongation

to fracture) in comparison with strength properties, due to the induced embrittlement, even for small precipitated weight fractions; i.e. in the case of samples hot deformed at 1100°C (HD 3) and solution treated at 1000°C with a treatment duration from 20min (ST 3.1.1) to 60min (ST 3.1.1) it can be noticed a significant decrease in elongation to fracture from 66% (ST 3.1.1) to 37% (ST 3.1.3), while the ultimate tensile strength showed a smaller decrease, from 762MPa (ST 3.1.1) to 673MPa (ST 3.1.3).

- Generally, for a solution treatment temperature above the necessary threshold to assure the precipitation of the sigma (σ) phase, it can be observed that the strength and ductility properties are strictly related to the law of phase mixture and the Hall-Pech grain-size influence; the best combination of mechanical properties, high-strength – high ductility, is obtained for a solution treatment performed just above the precipitation threshold of the sigma (σ) phase (1050°C); i.e. an ultimate tensile strength close 793MPa and elongation to fracture close to 61% recorded in the case of HD 1 + ST 1.1.1, 793MPa and 61% in the case of HD 2 + ST 2.1.1, 764MPa and 65% in the case of HD 3 + ST 3.1.1 and, 735MPa and 80% in the case of HD 4 + ST 4.1.1;
- *Based on the obtained results in terms of microstructural and mechanical behaviour data, one can design a suitable thermomechanical processing route* consisting of two processing stages, firstly, dealing with the hot deformation processing and, secondly, dealing with the solution treatment processing, *to obtain a suitable combination of mechanical properties* consisting of both high-ductility and high-strength.

8.2. Personal contributions

In terms of novelty, a series of original/personal contributions resulting from this thesis can be summarized as follows:

- A complex literature study, focused on Super Duplex Stainless Steel (SDSS) alloy, mainly on S32760 / F55 alloy, containing roughly equal proportions of ferrite/austenite phases, focused on the most influential thermomechanical processing parameters (combining mechanical and thermal processing), aiming to obtain a suitable combination of mechanical properties.
- Development of an original experimental program, considering the existing laboratory infrastructure in the University POLITEHNICA of Bucharest, to achieve the assumed objectives.
- Investigation of the effects induced by hot deformation, in the S32760 / F55 alloy, in the experimental space of deformation temperatures ranging from 1000°C to 1150°C.
- Investigation of the effects induced by the solution treatment on the microstructure and the exhibited mechanical properties, in a wide range of treatment temperatures ranging from 1000°C to 1100°C, with solution treatment durations ranging from 20mins to 60mins.
- Obtaining proper thermomechanically processed S32760 / F55 alloy samples, to be used in assessing the processing induced effects on the developed microstructure and mechanical properties.
- Development of specific investigation and characterization procedures, focused on S32760 / F55 alloy, to obtain confident data about the microstructure and the mechanical properties, by SEM, tensile and microhardness testing.

8.3. Recommendations

The performed experiments, focused on S32760 / F55 alloy, have shown that it is possible to obtain a suitable combination of mechanical properties (i.e., high strength and high ductility) when an appropriate thermomechanical processing route is applied. The following general recommendations can be made:

- When the objective is only to deform the S32760 / F55 alloy, the hot deformation processing must be performed at temperatures between 1050°C – 1100°C, to avoid the formation of the deleterious σ phase and to maximize the ductility properties (i.e., at 1050°C no σ-phase was detected and the ductility – expressed by the elongation to fracture – reached the maximum value of approx. 50±2%). At higher deformation temperatures (> 1100°C) one must also consider the induced decrease in the ductility due to the γ → δ phase transition.
- When the objective is to heat treat the S32760 / F55 alloy and to obtain the final desired mechanical properties (i.e., high strength and/or high-ductility properties), then the solution treatment must be performed at a temperature above 1000°C, in order to avoid formation of the deleterious σ phase. The ideal solution treatment temperature is situated close to 1050°C with a treatment duration of 20min when both high strength and high-ductility properties are obtained.
- When the maximum strength or ductility properties are envisaged the thermomechanical processing route must be performed as follows:
    - The highest ultimate tensile strength, close to 793±8MPa, was obtained in the case of hot-rolled at 1050°C (HR2) and solution treated at 1050°C for 20mins and WQ (ST 2.2.1) state.
    - The highest elongation to fracture, close to 80±5%, was obtained in the case of hot-rolled at 1150°C (HR4) and solution treated at 1050°C for 20mins and WQ (ST 4.2.1) state.

8.4. Future research directions

The future directions to continue the research in the field of thermomechanical processing and characterization of SDSS alloys can be summarized as follows:

- In addition to conventional examination methods, other advanced investigation techniques, such as: X-ray diffraction (XRD), transmission electron microscopy (TEM), etc, to accurately study the occurred microstructural changes within the alloy's microstructure (constituent phases, phase morphology, crystallography, etc.), precipitation of secondary phases, etc., to give insights into understanding the relationship between the microstructure and the exhibited mechanical properties.
- In addition to considering solution treatment processing parameters (treatment temperature and treatment duration), one may also consider the influence of cooling conditions, which can introduce a new level of complexity to the analysis procedure.
- The possibility to expand the thermomechanical processing routes with additional processing steps, i.e., ageing treatments may give rise to a better combination of strength/ductility properties, thus expanding the possible end-user applications.

Selected References

[1]. Cobb, Harold M.; *The History of Stainless Steel. Materials Park*, OH: ASM International. (2010). Retrieved 8 March 2020.

[2]. Peckner,; Donald; Bernstein,; McGraw Hill,; I.M. *Handbook of Stainless Steels*, 1997.

[3]. Lacombe, P.; Baroux, B.; Beranger, G. *Les Aciers Inoxydables*. Les Editions de Physique, 1990.

[4]. Davis, Joseph R.(ed.) (1994). *Stainless Steels ASM Specialty Handbook. Materials Park*.; OH: ASM International. Retrieved 8 March 2020.

[13]. L. E. Newton.; R. H. Hausler.; *Methodology to Study Cost of Corrosion.* Corrosion Engineering, Science and Technology, University of Cantabria, Spain.; Vol. 40, No. 4.; Dec. 2005.

[14]. M. G. Fontana.; *Corrosion Engineering*. Third Edition, McGraw Hill, New York 1987.

[15]. S. Bradford.; *Corrosion Control*. Second Edition, Casti Publishing Inc. Alberta, Canada, 2003.

[16]. Peckner, Donald; Bernstein, I.M.; *Handbook of Stainless Steels*.; chapter 8.; McGraw Hill. (1977)

[17]. R. M. R. Davison.; *Practical Guide to Using Duplex Stainless Steels*. Material Performance, 1990. 29(1): pp. 57-62.

[18]. J.-O. Nilsson.; P. Kangas.; T. Karlsson.; A. Wilson.; *Mechanical properties, microstructural stability and kinetics of σ-phase formation in 29Cr-6Ni-2Mo-0.38N super duplex stainless steel*. Metallurgical and Materials Transactions A. Vol. 31, No. 1, Jan 2000, pp. 35-45.

[79]. Davison, Ralph M.; and James D. Redmond.; Practical Guide to Using Duplex Stainless Steels. *Materials Performance*, January 1990, pp. 57-62.

[80]. Degarmo, E. Paul; Black, J. T.; Kohser, Ronald A. *Materials and Processes in Manufacturing* (11th ed.). Wiley, 2011.

[81]. *Heavy Manufacturing of Power Plants World Nuclear Association, September 2010*. Retrieved: 25 September 2010.

[112]. Ayorinde Tayo e.t al. Data sets on the measurement of mechanical properties of ferrite and austenite constitutive phases using nanoindentation and micro hardness techniques. A.T. Olanipekun et al.; *Data in brief* 27 (2019) 1045512.

[113]. C. Meena, V. Uthaisangsuk. Micromechanics Based Modeling of Effect of Sigma Phase on Mechanical and Failure Behavior of Duplex Stainless Steel. *Metallurgical and Materials Transactions*, A volume 52, pages1293–1313 (2021).

[114]. Elisabeta Mirela Cojocaru, et, al. Influence of ageing treatment on microstructural and mechanical properties of a solution treated UNS S32750/EN 1.4410/F53 Super Duplex Stainless Steel (SDSS) alloy. *Journal of Materials Research and Technology;* Volume 9, Issue 4, July–August 2020, Pages 8592-8605.

[115]. Kai Wang Chan and Sie Chin Tjong. Effect of Secondary Phase Precipitation on the Corrosion Behavior of Duplex Stainless Steels. *Materials* 2014, 7, 5268-5304; doi:10.3390/ma7075268.

Results dissemination

A) Published scientific papers within a journal with high impact factor (IF):

1. Elisabeta Mirela COJOCARU, Doina RADUCANU, **Saleh Sabah ALTURAIHI**, Anna NOCIVIN, George COMAN and Vasile Danut COJOCARU. *Influence Of Isochronal Treatments on Microstructure and Mechanical Properties of Solution Treated UNS S32750 SDSS Alloy Specimens*, ***Journal of Materials Research and Technology*** *Volume 9, Issue 4, July–August 2020, Pages 7870-7879.*
2. Elisabeta Mirela COJOCARU, Doina RADUCANU, Adrian Nicolae VINTILA, **Saleh Sabah ALTURAIHI**, Nicolae SERBAN, Andrei Constantin BERBECARU and Vasile Danut COJOCARU. *Influence of ageing treatment on microstructural and mechanical properties of a solution treated UNS S32750/EN 1.4410/F53 Super Duplex Stainless Steel (SDSS) alloy*, ***Journal of Materials Research and Technology*** *Volume 9, Issue 4, July–August 2020, Pages 8592-8605.*

B) Published scientific papers within ISI journal:

1. **Saleh Sabah ALTURAIHI**, Mohammed Hayder ALLUAIBI, Elisabeta Mirela COJOCARU and Doina RADUCANU. *Microstructural changes occurred during hot-deformation of SDSS F55 (super-duplex stainless steel) alloy*, ***University Politehnica of Bucharest Scientific Bulletin Series B - Chemistry and Materials Science***, 2019, Vol. 81, No. 1, pp. 149-160.
2. Mohammed Hayder ALLUAIBI, **Saleh Sabah ALTURAIHI**, Elisabeta Mirela COJOCARU and Ion CINCA. *Microstructural evolution during thermomechanical processing of Ti-6246 titanium alloy*, ***University Politehnica of Bucharest Scientific Bulletin: Series B - Chemistry and Materials Science***, 2019, Vol. 81, No. 1, pp. 225-234.
3. **Saleh Sabah ALTURAIHI**, Nicolae SERBAN, Ion CINCA, Mariana Lucia ANGELESCU and Irina Varvara BALKAN. *Influence Of Solution Treatment Temperature on Microstructural and Mechanical Properties of Hot Rolled UNS S32760 / F55 Super Duplex Stainless Steel (SDSS)*, ***University Politehnica of Bucharest Scientific Bulletin Series B - Chemistry and Materials Science,*** 2021, Vol. 83, No. 3, pp. 275-284.
4. Mohammed Hayder ALLUAIBI, **Saleh Sabah ALTURAIHI**, Adrian RUSEA, Elisabeta Mirela COJOCARU. *The response of microstructure and mechanical properties of Ti-6246 alloy to thermomechanical processing*, ***University Politehnica of Bucharest Scientific Bulletin: Series B - Chemistry and Materials Science***, 2021, Vol. 83, No. 2, pp. 231-242.

C) Published scientific papers in international conferences within the index of Scopus and Clarivate:

1. Mohammed Hayder ALLUAIBI, **Saleh Sabah ALTURAIHI**, Doina RADUCANU, Adrian RUSEA, Ion CINCA, Anna NOCIVIN, Vasile Danut COJOCARU. *Microstructure investigation and mechanical properties of Ti-6Al-2Sn-4Zr-6Mo alloy processed by hot rolling and solution treatment*, ***Metal***, Brno, Czech Republic, 2020.